Chapter 7

Scattering from complex potentials

So far we have discussed the scattering of structureless particles off real potentials. In most applications in the physical world, one deals with collisions of molecular, atomic or nuclear system, where the process of scattering is very complicated. Such situations require the introduction of new concepts, which will be expanded upon in the second part of this book. A first step in this direction is the generalization of the interaction potential into a complex one. This potential enables us to describe some features of the elastic scattering of composite particles. The imaginary part of this interaction mocks up the loss of flux into non-elastic processes. A fuller description of the complex potential (usually called the Optical Potential) using a microscopic treatment of the collision process will be developed later. In the following, we simply take the interaction to be complex and seek the consequences in so far as the elastic scattering observables are concerned. We also generalize the formal scattering theory (T-matrix, S-matrix, etc.) to this new frontier.

7.1   The absorption cross section

Since the Hamiltonian is usually Hermitian, the total current,

$$\mathbf{j} = \frac{\hbar}{2\mu i} \left[\psi^* \left(\mathbf{r} \right) \nabla \psi \left(\mathbf{r} \right) - \psi \left(\mathbf{r} \right) \nabla \psi^* \left(\mathbf{r} \right) \right], \qquad (7.1)$$

satisfies the continuity equation, which for a stationary state is

$$\nabla \cdot \mathbf{j} = 0 \,.$$

However, this is not valid for complex potentials. In this case, the Hamiltonian has the form [Feshbach (1962)]

Scattering Theory of Molecules, Atoms and Nuclei

$$H = -\frac{\hbar^2}{2\mu}\nabla^2 + V(r), \qquad \text{with} \qquad V(r) = U(r) + i\,W(r), \qquad (7.2)$$

where $U(r)$ is real and $W(r)$ is a short range negative[1] function of r. The term $i\,W$ takes care of the flux lost to excited channels. A peculiar aspect of H which is brought to light is that, naively, one may imagine that its energy spectrum will be complex. However, the energy eigenvalue is implicitly that of the exact many-channel problem (see chapter 9) with a real interaction. The imaginary complex potential comes about through the process of reducing the coupled channel equations to a single effective equation for the elastic channel, with a complex potential (see part II). Nevertheless, the energy has the same real value as the one appearing in the original set of coupled equations.

In the case of complex potentials, the continuity equation must be modified. For this purpose, we write the Schrödinger equation and its complex conjugate,

$$\left[-\frac{\hbar^2}{2\mu}\nabla^2 + U(r) + i\,W(r) \right] \psi(\mathbf{r}) = E\,\psi(\mathbf{r}) \qquad (7.3)$$

$$\left[-\frac{\hbar^2}{2\mu}\nabla^2 + U(r) - i\,W(r) \right] \psi^*(\mathbf{r}) = E\,\psi^*(\mathbf{r}), \qquad (7.4)$$

and evaluate $\psi^*(\mathbf{r}) \times$ Eq. (7.3) - $\psi(\mathbf{r}) \times$ Eq. (7.4). The resulting equation can be written

$$\frac{\hbar}{2\mu i}\left[\psi^*(\mathbf{r})\,\nabla^2\,\psi(\mathbf{r}) - \psi(\mathbf{r})\,\nabla^2\,\psi^*(\mathbf{r}) \right] = \frac{2}{\hbar}\,W(r)\,|\psi(\mathbf{r})|^2, \qquad (7.5)$$

or, identifying the LHS of Eq. (7.5) as the divergence of the total current,

$$\nabla \cdot \mathbf{j} = \frac{2}{\hbar}\,W(\mathbf{r})\,|\psi(\mathbf{r})|^2. \qquad (7.6)$$

Eq. (7.6) can be put in an integral form. For this purpose, we integrate it over the volume of a large sphere, which encloses the region of non-vanishing absorption $(W(\mathbf{r}) \neq 0)$. We get

---

[1]If the optical potential is derived from coupled-channel equations (see part II of this book), it is non-local and state-dependent. In such situations it may be replaced by a local effective potential which leads to the same elastic wave function. This potential may have a positive imaginary part within some $r-$range. However, the overall effect of this potential must be that of a sink of flux.

$$\int d^3\mathbf{r} \ \nabla \cdot \mathbf{j} = \frac{2}{\hbar} \int d^3\mathbf{r} \ W(r) \ \ |\psi(\mathbf{r})|^2 ,$$

or, using the divergence theorem,

$$\int d\mathbf{s} \cdot \mathbf{j} = \frac{2}{\hbar} \int d^3\mathbf{r} \ W(r) \ \ |\psi(\mathbf{r})|^2 . \tag{7.7}$$

This result can be used to obtain the absorption cross section in a scattering problem. In this case, the wave function, $\psi^{(+)}$, has scattering boundary conditions and

$$N_a = - \int d\mathbf{s} \cdot \mathbf{j}$$

is the number of absorbed particles per unit time. The absorption cross section is then obtained dividing N_a by the incident flux $J = |A|^2 v$ (Eq. (1.68)). We get

$$\sigma_a = \left(\frac{1}{|A|^2}\right) \frac{2}{\hbar v} \int d^3\mathbf{r} \ [-W(r)] \ \ |\psi^{(+)}(\mathbf{r})|^2 . \tag{7.8}$$

Note that the wave function $\psi^{(+)}$ contains the full effect of W. Writing v in terms of E and k and using a more compact notation, Eq. (7.8) takes the form

$$\sigma_a = \frac{1}{|A|^2} \ \times \ \frac{k}{E} \ \left\langle \psi^{(+)} \right| \ \left[-W(r) \right] \ \left| \psi^{(+)} \right\rangle . \tag{7.9}$$

Some authors (e.g. [Satchler *et al.* (1987)]) normalizes $\psi_{\mathbf{k}}^{(+)}$ such that it has the asymptotic behavior (Eq. (1.61) with $A = 1$)

$$\psi_{\mathbf{k}}^{(+)}(\mathbf{r}) \to e^{i\mathbf{k}\cdot\mathbf{r}} \ + \ f(\Omega) \frac{e^{ikr}}{r} . \tag{7.10}$$

In this case, Eq. (7.9) takes the simpler form

$$\sigma_a = \frac{k}{E} \ \left\langle \psi^{(+)} \middle| W \middle| \psi^{(+)} \right\rangle . \tag{7.11}$$

It should be stressed that the above equation is not valid for the normalization constant $A = (2\pi)^{-3/2}$, adopted in the present text. The absorption cross section is then given by Eq. (7.9).

The absorption cross section is a very inclusive piece of information. It gives the total flux removed from the elastic channel, without specifying

312   *Scattering Theory of Molecules, Atoms and Nuclei*

how it is distributed over the open channels. Eq. (7.9) becomes particularly useful when the absorptive potential is a sum of terms[2], $W = W_1 + W_2 + ..$, each one associated with the coupling with one specific channel. In this case, the cross section for the corresponding channel, i, can be estimated by Eq. (7.9), with the same wave function but with the replacement $W \to W_i$.

For practical purposes, σ_a can be expressed in terms of radial integrals. Using in Eq. (7.9) the partial-wave expansion of the wave function (Eq. (2.57a)) and the orthogonality relation for the Legendre Polynomials (Eq. (2.60)), we obtain the result

$$\sigma_a = \frac{\pi}{k^2} \sum_l (2l+1) \, \mathcal{T}_l \,, \qquad (7.12)$$

where $\mathcal{T}_l$ is the absorption coefficient at the partial-wave l,

$$\mathcal{T}_l = \frac{4k}{E} \int_0^\infty dr \, \left[-W(r) \right] \left| u_l(k,r) \right|^2 . \qquad (7.13)$$

It can be easily shown that the absorption coefficients are related to the $l-$components of the S-matrix as

$$\mathcal{T}_l = 1 - |S_l|^2 \ . \qquad (7.14)$$

For this purpose, we evaluate (see section (1.5))

$$\sigma_a \equiv \frac{N_a}{J} = -\frac{1}{v} \int d\mathbf{s} \cdot \mathbf{j} = -\frac{r^2}{v} \int d\Omega \ j_r \,, \qquad (7.15)$$

where j_r is the radial component of the total current,

$$\begin{aligned} j_r &= \frac{\hbar}{2\mu i} \left[\left(\psi_{\mathbf{k}_i}^{(+)}\right)^* \frac{\partial}{\partial_r} \left(\psi_{\mathbf{k}_i}^{(+)}\right) - \psi_{\mathbf{k}_i}^{(+)} \frac{\partial}{\partial_r} \left(\psi_{\mathbf{k}_i}^{(+)}\right)^* \right] \\ &= \frac{\hbar}{\mu} \, \mathrm{Im} \left\{ \left(\psi_{\mathbf{k}_i}^{(+)}\right)^* \frac{\partial}{\partial_r} \left(\psi_{\mathbf{k}_i}^{(+)}\right) \right\} . \end{aligned} \qquad (7.16)$$

To calculate j_r, we recall Eq. (2.50);

$$\psi_{\mathbf{k}}^{(+)} = X_- \, \frac{e^{-ikr}}{r} + X_+ \, \frac{e^{ikr}}{r} \,. \qquad (7.17)$$

Using the expressions for $X_\pm$ (Eqs.(2.48) and (2.47)) with the coefficients C_l of Eq. (2.45), we can write

---

[2]The derivation of these potentials is given in chapter 9

$$X_- = -\sum_l \frac{2l+1}{2ik} \ (-)^l \ P_l(\cos\theta) \tag{7.18}$$

$$X_+ = \sum_l \frac{2l+1}{2ik} \ S_l \ P_l(\cos\theta) \ . \tag{7.19}$$

Inserting Eq. (7.17) into Eq. (7.16), we obtain

$$j_r = \frac{v}{r^2} \ \left(|X_+|^2 - |X_-|^2\right) \ .$$

Using this result in Eq. (7.15), we get

$$\sigma_a = \int d\Omega \ |X_-|^2 - \int d\Omega \ |X_+|^2 \ .$$

Above, the first integral represents the flux of the incident spherical wave while the second integral gives the corresponding emergent flux. The explicit form of $X_\pm$ (Eqs. (7.18) and (7.19)) together with the orthogonality relation for the Legendre Polynomials (Eq. (2.60)) lead to the result

$$\sigma_a = \frac{\pi}{k^2} \ \sum_l (2l+1) \ \left[1 - |S_l|^2\right] \ . \tag{7.20}$$

Note that for real potentials $|S_l| = 1$ and σ_a vanishes. Comparing Eqs. (7.20) and (7.12), we have the proof of Eq. (7.14).

An interesting limit, discussed further in chapter 5, is the Born approximation. In this case, the wave function $\psi^{(+)}$ is replaced by a plane wave and thus the absorption cross section of Eq. (7.9) becomes simply

$$\sigma_a = \frac{k}{E} \ \int d^3\mathbf{r} \ [-W(r)] \ . \tag{7.21}$$

If we further take $W(r)$ to be a step function, namely

$$W(r) = -W_0 \ \Theta(\bar{R} - r),$$

where $\bar{R}$ is the absorption range and W_0 (a positive quantity) is the strength of the absorptive potential, we get the simple expression

$$\sigma_a = \frac{4\pi k}{3E} \ W_0 \bar{R}^3 = \left(\frac{8\pi W_0 \bar{R}^3}{3\hbar}\right) \frac{1}{v} \ . \tag{7.22}$$

Thus, the above approximation gives an absorption cross section which goes inversely with the velocity of the absorbed particle. This behavior is in fact

314   *Scattering Theory of Molecules, Atoms and Nuclei*

observed in very low energy neutron scattering from nuclei as well as in atoms, where the phenomenon is refered to as *Wigner's law*. We should warn the reader that in these systems the Born approximation is not valid and the above result should be considered as a mere coincidence.

To close this section we show the generalization of the Optical Theorem for complex potentials. The essential difference is that for them $|S_l| < 1$. In this case, we get

$$\frac{4\pi}{k}\mathrm{Im}\left\{f(0)\right\} = \frac{2\pi}{k^2} \sum_l (2l+1) \left[1 - \mathrm{Re}\left\{S_l\right\}\right]. \qquad (7.23)$$

It is straightforward to check that the same result is obtained summing Eqs. (7.20) and (2.61a). Therefore, the Optical Theorem for complex potentials becomes

$$\sigma_{\mathrm{el}} + \sigma_a = \frac{4\pi}{k}\mathrm{Im}\left\{f(0)\right\} . \qquad (7.24)$$

Special care is required when use is made of Eq. (7.24) for charged particle scattering. In this case the Coulomb interaction renders σ_{el} infinite. In such situations, one relies on the two-potential formula for the scattering amplitude (see section 4.5),

$$f(\theta) = f_{\mathrm{C}}(\theta) + \bar{f}(\theta) , \qquad (7.25)$$

where $f_{\mathrm{C}}(\theta)$ is the Coulomb scattering amplitude (Eq. (3.29)) and $\bar{f}(\theta)$ is the correction owing to the short range complex potential. Carrying out the partial-wave expansion for $\bar{f}(\theta)$, we get (see section 3.4)

$$\bar{f}(\theta) = \frac{1}{2ik} \sum_l (2l+1)\, e^{2i\sigma_l} \left[e^{2i\,\bar{\delta}_l} - 1\right] . \qquad (7.26)$$

Above, σ_l are the Coulomb phase shift and $\bar{\delta}_l$ is the complex phase shift arising from the short range complex potential. The cross section $d\sigma/d\Omega$ can be related to the Coulomb cross section $d\sigma_{\mathrm{C}}/d\Omega$ as

$$\frac{d\sigma}{d\Omega} - \frac{d\sigma_{\mathrm{C}}}{d\Omega} = \left|\bar{f}(\theta)\right|^2 + 2\mathrm{Re}\left\{f_{\mathrm{C}}^*(\theta)\,\bar{f}(\theta)\right\} . \qquad (7.27)$$

Following Holdeman and Thaler [Holdeman and Thaler (1965)], a modified Optical Theorem can be obtained by integrating the above equation in the range $\theta_0 < \theta < \pi$, with θ_0 chosen to be very small. This procedure, known as the *Sum-of-Differences Method* (SOD), results in an expression which

is convenient for the extraction of the σ_a. The SOD form of the Optical Theorem can be written as

$$
\sigma_a + 2\pi \int_{\theta_0}^{\pi} d\theta \, \sin\theta \left(\frac{d\sigma}{d\Omega} - \frac{d\sigma_{\mathrm{C}}}{d\Omega} \right)
$$
$$
= \frac{4\pi}{k} \left| \bar{f}(\theta_0) \right| + \sin \left[\arg \left(\bar{f}(\theta_0) \right) - 2\sigma_0 + 2\eta \ln \left(\sin \theta_0 / 2 \right) \right]. \quad (7.28)
$$

Eq. (7.28) is the appropriate form of the Optical Theorem used in the analysis of the elastic scattering of charged particles in the presence of absorption.

7.2 Lippmann-Schwinger equations with complex potentials

If the potential is complex, an extension of the dimension of the Hilbert space is required. Since $H = H_0 + V$ and $H^\dagger = H_0 + V^\dagger$ are different, one needs to introduce bi-orthogonal sets of scattering wave functions for each boundary condition.

In chapter 4 we have shown that the relevant quantities in Scattering Theory are contained in the state $|\psi_{\mathbf{k}}^{(+)}\rangle$ or, alternatively, in $|\psi_{\mathbf{k}}^{(-)}\rangle$, which is obtained from the $|\psi_{-\mathbf{k}}^{(+)}\rangle$ through the time-reversal operation (see section (4.3.3)). They are both solutions of the equation

$$
\left[E_k - H \right] \left| \psi_{\mathbf{k}}^{(\pm)} \right\rangle = 0, \quad (7.29)
$$

with different boundary conditions. When $H \neq H^\dagger$, the situation is more complicated. The physical state

$$
\left| \psi_{\mathbf{k}}^{(-)} \right\rangle = \mathbb{T} \left| \psi_{-\mathbf{k}}^{(+)} \right\rangle, \quad (7.30)
$$

where $\mathbb{T}$ is the time-reversal operator, is no longer a solution of Eq. (7.29) but satisfies the equation

$$
\left[E_k - H^\dagger \right] \left| \psi_{\mathbf{k}}^{(-)} \right\rangle = 0. \quad (7.31)
$$

It may look unreasonable that the physical state $\psi_{\mathbf{k}}^{(-)}$ satisfies a Schrödinger equation with the Hamiltonian $H^\dagger$, which acts as a source. However, one should have in mind that calculations of the S- and the T-matrix elements involve $\left(\psi_{\mathbf{k}}^{(-)}(\mathbf{r}) \right)^*$, which satisfies an equation with H.

Following the same procedures as in chapter 4 but starting from Eqs. (7.29) (for $|\psi_{\mathbf{k}}^{(+)}\rangle$) and (7.31) (for $|\psi_{\mathbf{k}}^{(-)}\rangle$), one obtains the Lippmann-Schwinger equations

$$|\psi_{\mathbf{k}}^{(+)}\rangle = |\phi_{\mathbf{k}}\rangle + G_0^{(+)}(E_k)\, V\, |\psi_{\mathbf{k}}^{(+)}\rangle = |\phi_{\mathbf{k}}\rangle + G^{(+)}(E_k) V\, |\phi_{\mathbf{k}}\rangle \quad (7.32)$$

$$|\psi_{\mathbf{k}}^{(-)}\rangle = |\phi_{\mathbf{k}}\rangle + G_0^{(-)}(E_k)\, V^\dagger\, |\psi_{\mathbf{k}}^{(-)}\rangle = |\phi_{\mathbf{k}}\rangle + G^{(-)}(E_k) V^\dagger\, |\phi_{\mathbf{k}}\rangle\,, (7.33)$$

where $G_0^{(\pm)}$ are the free particle Green's functions of chapter 4 and $G^{(\pm)}$ are given by

$$G^{(+)}(E_k) = \frac{1}{E_k - H + i\epsilon}, \qquad (7.34)$$

$$G^{(-)}(E_k) = \frac{1}{E_k - H^\dagger - i\epsilon}\,. \qquad (7.35)$$

Note that the property (see Eq. (4.31)) $G^{(\pm)}(E_k) = \left[G^{(\mp)}(E_k)\right]^\dagger$ is still valid.

For complex potentials, the states $|\psi_{\mathbf{k}}^{(+)}\rangle$ no longer form an orthogonal set. That is, $\langle\psi_{\mathbf{k}'}^{(+)}|\psi_{\mathbf{k}}^{(+)}\rangle \neq \delta(\mathbf{k}-\mathbf{k}')$. The same occurs with the set of states $|\psi_{\mathbf{k}}^{(-)}\rangle$. However, one can introduce appropriate *dual* states $|\tilde{\psi}_{\mathbf{k}}^{(+)}\rangle$ and $|\tilde{\psi}_{\mathbf{k}'}^{(-)}\rangle$ which do satisfy the orthonormality conditions

$$\langle\tilde{\psi}_{\mathbf{k}}^{(+)}|\psi_{\mathbf{k}'}^{(+)}\rangle = \delta(\mathbf{k} - \mathbf{k}'), \qquad (7.36)$$

$$\langle\psi_{\mathbf{k}'}^{(-)}|\tilde{\psi}_{\mathbf{k}}^{(-)}\rangle = \delta(\mathbf{k} - \mathbf{k}'). \qquad (7.37)$$

The completeness relations should be modified accordingly, taking the form

$$\int |\psi_{\mathbf{k}}^{(+)}\rangle \, d^3\mathbf{k} \, \langle\tilde{\psi}_{\mathbf{k}}^{(+)}| + P_{\mathrm{B}} = \mathbf{1}, \qquad (7.38)$$

$$\int \left|\tilde{\psi}_{\mathbf{k}}^{(-)}\right\rangle \, d^3\mathbf{k} \, \langle\psi_{\mathbf{k}}^{(-)}| + P_{\mathrm{B}} = \mathbf{1}, \qquad (7.39)$$

with the term P_{B} accounting for the bound states of the potential.

The dual states are defined by their Lippmann-Schwinger equations[3],

---

[3]The proof that the dual states $|\tilde{\psi}_{\mathbf{k}}^{(+)}\rangle$ and $|\tilde{\psi}_{\mathbf{k}'}^{(-)}\rangle$, defined by Eqs. (7.41) and (7.43), are respectively orthogonal to $|\psi_{\mathbf{k}'}^{(+)}\rangle$ and $|\psi_{\mathbf{k}'}^{(-)}\rangle$ is analogous to that given in section 4.1 for real potentials.

Scattering from complex potentials   317

$$\left|\tilde{\psi}_{\mathbf{k}}^{(+)}\right\rangle = \left|\phi_{\mathbf{k}}\right\rangle + G_0^{(+)}(E_k)\, V^\dagger \left|\tilde{\psi}_{\mathbf{k}}^{(+)}\right\rangle \qquad (7.40)$$

$$= \left|\phi_{\mathbf{k}}\right\rangle + \tilde{G}^{(+)}(E_k) V^\dagger \left|\phi_{\mathbf{k}}\right\rangle, \qquad (7.41)$$

and

$$\left|\tilde{\psi}_{\mathbf{k}}^{(-)}\right\rangle = \left|\phi_{\mathbf{k}}\right\rangle + G_0^{(-)}(E_k)\, V \left|\tilde{\psi}_{\mathbf{k}}^{(-)}\right\rangle \qquad (7.42)$$

$$= \left|\phi_{\mathbf{k}}\right\rangle + \tilde{G}^{(-)}(E_k) V \left|\phi_{\mathbf{k}}\right\rangle, \qquad (7.43)$$

where the dual full Green's functions $\tilde{G}^{(\pm)}$ are

$$\tilde{G}^{(+)}(E_k) = \frac{1}{E_k - H^\dagger + i\epsilon}, \qquad (7.44)$$

$$\tilde{G}^{(-)}(E_k) = \frac{1}{E_k - H - i\epsilon}. \qquad (7.45)$$

Multiplying Eqs. (7.41) and (7.43) from the left by the operators $(E - H_0 + i\epsilon)$ and $(E - H_0 + i\epsilon)$, respectively, and rearranging terms, we obtain the Schrödinger equations for the dual states

$$\left(E_k - H^\dagger\right) \left|\tilde{\psi}_{\mathbf{k}}^{(+)}\right\rangle = 0,$$
$$\left(E_k - H\right) \left|\tilde{\psi}_{\mathbf{k}}^{(-)}\right\rangle = 0.$$

The physical scattering wave functions $\psi_{\mathbf{k}}^{(\pm)}$ and their dual partners $\tilde{\psi}_{\mathbf{k}}^{(\pm)}$ can now be used to generate the spectral representations of Eqs. (7.34) and (7.35)

$$G^{(+)}(E_k) = \int \frac{\left|\psi_{\mathbf{q}}^{(+)}\right\rangle d^3\mathbf{q} \left\langle\tilde{\psi}_{\mathbf{q}}^{(+)}\right|}{E_k - E_q + i\epsilon} \qquad (7.46)$$

and

$$G^{(-)}(E_k) = \int \frac{\left|\tilde{\psi}_{\mathbf{q}}^{(-)}\right\rangle d^3\mathbf{q} \left\langle\psi_{\mathbf{q}}^{(-)}\right|}{E_k - E_q - i\epsilon}. \qquad (7.47)$$

The spectral representations of $\tilde{G}^{(\pm)}$ can be obtained analogously.

In chapter 4, we used the explicit form of the free Green's function (Eq. (4.37)) in the Lippmann-Schwinger equation for $\psi_{\mathbf{k}}^{(+)}(\mathbf{r})$ to get the asymptotic form of the scattering function. The asymptotic form of $\psi_{\mathbf{k}}^{(-)}(\mathbf{r})$ was then obtained from the property $\left(\psi_{\mathbf{k}}^{(-)}(\mathbf{r})\right)^* = \psi_{-\mathbf{k}}^{(+)}(\mathbf{r})$. Analogous

Scattering Theory of Molecules, Atoms and Nuclei

procedures can be used to derive the asymptotic form of $\psi_{\mathbf{k}}^{(\pm)}(\mathbf{r})$. The results are summarized below

$$\psi_{\mathbf{k}}^{(+)}(\mathbf{r}) \to A \left(e^{i\mathbf{k}\cdot\mathbf{r}} + f(\theta) \, \frac{e^{ikr}}{r} \right), \tag{7.48}$$

$$\psi_{\mathbf{k}}^{(-)}(\mathbf{r}) \to A \left(e^{i\mathbf{k}\cdot\mathbf{r}} + f^*(\pi - \theta) \, \frac{e^{-ikr}}{r} \right), \tag{7.49}$$

$$\tilde{\psi}_{\mathbf{k}}^{(+)}(\mathbf{r}) \to A \left(e^{i\mathbf{k}\cdot\mathbf{r}} + \tilde{f}(\theta) \, \frac{e^{ikr}}{r} \right), \tag{7.50}$$

$$\tilde{\psi}_{\mathbf{k}}^{(-)}(\mathbf{r}) \to A \left(e^{i\mathbf{k}\cdot\mathbf{r}} + \tilde{f}^*(\pi - \theta) \, \frac{e^{-ikr}}{r} \right), \tag{7.51}$$

with

$$f(\theta) = -2\pi^2 \left(\frac{2\mu}{\hbar^2} \right) \left\langle \phi_{\mathbf{k}'} \left| V \right| \psi_{\mathbf{k}}^{(+)} \right\rangle \tag{7.52}$$

$$\tilde{f}(\theta) = -2\pi^2 \left(\frac{2\mu}{\hbar^2} \right) \left\langle \phi_{\mathbf{k}'} \left| V^\dagger \right| \tilde{\psi}_{\mathbf{k}}^{(+)} \right\rangle. \tag{7.53}$$

We have demonstrated above that the complex nature of the potential leads to a deviation of the scalar products $\langle \psi_{\mathbf{k}}^{(+)} | \psi_{\mathbf{k}'}^{(+)} \rangle$ from the Dirac's delta function. Now we explicitly evaluate this deviation. We first relate $\psi_{\mathbf{k}}^{(+)}$ to $\tilde{\psi}_{\mathbf{k}}^{(+)}$ through a Lippmann-Schwinger like equation. Using the relation

$$H^\dagger = H - V + V^\dagger$$

in Eq. (7.29) we can write

$$\left(E_k - H^\dagger \right) |\psi_{\mathbf{k}}^{(+)}\rangle = \left(V - V^\dagger \right) |\psi_{\mathbf{k}}^{(+)}\rangle. \tag{7.54}$$

This equation can be formally solved as

$$|\psi_{\mathbf{k}}^{(+)}\rangle = |\tilde{\psi}_{\mathbf{k}}^{(+)}\rangle + \tilde{G}^{(+)}(E_k) \left(V - V^\dagger \right) |\psi_{\mathbf{k}}^{(+)}\rangle. \tag{7.55}$$

Formal manipulation of this equation together with the orthogonality relation of Eq. (7.36) leads to

$$\langle \psi_{\mathbf{k}'}^{(+)} | \psi_{\mathbf{k}}^{(+)} \rangle = \delta(\mathbf{k} - \mathbf{k}') + \frac{\langle \psi_{\mathbf{k}'}^{(+)} | \left(V - V^\dagger \right) | \psi_{\mathbf{k}}^{(+)} \rangle}{E_k - E_{k'} + i\epsilon}. \tag{7.56}$$

A similar relation can be obtained for the scalar product $\langle \psi_{\mathbf{k}'}^{(-)} | \psi_{\mathbf{k}}^{(-)} \rangle$, following the same procedures as above. The result is

$$\langle \psi_{\mathbf{k}'}^{(-)} | \psi_{\mathbf{k}}^{(-)} \rangle = \delta(\mathbf{k} - \mathbf{k}') + \frac{\langle \psi_{\mathbf{k}'}^{(-)} | \left(V^\dagger - V \right) | \psi_{\mathbf{k}}^{(-)} \rangle}{E_k - E_{k'} - i\epsilon} \,. \tag{7.57}$$

The matrix-elements $\langle \psi_{\mathbf{k}'}^{(-)} | \left(V^\dagger - V \right) | \psi_{\mathbf{k}}^{(-)} \rangle$ can be reduced to those appearing in Eq. (7.56). For this purpose we use Eq. (7.30) written in the form

$$|\psi_{\mathbf{k}}^{(-)}\rangle = \mathbb{T} |\psi_{-\mathbf{k}}^{(+)}\rangle = \mathbb{T}\mathbb{R} |\psi_{\mathbf{k}}^{(+)}\rangle$$

where $\mathbb{R}$ is the space reflection operator. We obtain

$$\begin{aligned}
\langle \psi_{\mathbf{k}'}^{(-)} | \left(V^\dagger - V \right) | \psi_{\mathbf{k}}^{(-)} \rangle &= \langle \psi_{\mathbf{k}'}^{(+)} | \mathbb{R}^\dagger \mathbb{T}^\dagger \left(V^\dagger - V \right) \mathbb{T}\mathbb{R} | \psi_{\mathbf{k}}^{(+)} \rangle \\
&= \langle \psi_{\mathbf{k}'}^{(+)} | \mathbb{R}^\dagger \left(V - V^\dagger \right) \mathbb{R} | \psi_{\mathbf{k}}^{(+)} \rangle \\
&= \langle \psi_{\mathbf{k}'}^{(+)} | \left(V - V^\dagger \right) | \psi_{\mathbf{k}}^{(+)} \rangle \,. \tag{7.58}
\end{aligned}$$

The last step was carried out as a consequence of the assumed space reflection invariance of the potential. Therefore, the only difference between Eqs. (7.56) and (7.57) is the sign of $i\epsilon$ in the denominator of the second term. Accordingly,

$$\begin{aligned}
\langle \psi_{\mathbf{k}'}^{(+)} | \psi_{\mathbf{k}}^{(+)} \rangle - \langle \psi_{\mathbf{k}'}^{(-)} | \psi_{\mathbf{k}}^{(-)} \rangle &= \left[\frac{1}{E_k - E_{k'} + i\epsilon} - \frac{1}{E_k - E_{k'} - i\epsilon} \right] \\
&\quad \times \langle \psi_{\mathbf{k}'}^{(+)} | \left(V - V^\dagger \right) | \psi_{\mathbf{k}}^{(+)} \rangle \,.
\end{aligned}$$

or

$$\begin{aligned}
\langle \psi_{\mathbf{k}'}^{(+)} | \psi_{\mathbf{k}}^{(+)} \rangle - \langle \psi_{\mathbf{k}'}^{(-)} | \psi_{\mathbf{k}}^{(-)} \rangle &= - \left[|A|^2 \, 4\pi \left(\frac{E_k}{k} \right) \delta \left(E_k - E_{k'} \right) \right] \\
&\quad \times \frac{1}{|A|^2} \frac{k}{E_k} \langle \psi_{\mathbf{k}'}^{(+)} | W | \psi_{\mathbf{k}}^{(+)} \rangle \,,
\end{aligned}$$

where $W = -\text{Im}\{V\}$. Since we are assuming the normalization of Eqs. (7.36) and (7.37), we should set $|A|^2 = (2\pi)^{-3}$ within the square brackets of the above equation. It then becomes

$$\begin{aligned}
\langle \psi_{\mathbf{k}'}^{(+)} | \psi_{\mathbf{k}}^{(+)} \rangle - \langle \psi_{\mathbf{k}'}^{(-)} | \psi_{\mathbf{k}}^{(-)} \rangle &= - \left[\frac{1}{2\pi^2} \left(\frac{E_k}{k} \right) \delta \left(E_k - E_{k'} \right) \right] \\
&\quad \times \frac{1}{|A|^2} \frac{k}{E_k} \langle \psi_{\mathbf{k}'}^{(+)} | W | \psi_{\mathbf{k}}^{(+)} \rangle \,. \tag{7.59}
\end{aligned}$$

Note that, with the constraint imposed by the delta function, the quantity

$$\Sigma_{\mathbf{k}',\mathbf{k}}^a \equiv \frac{1}{|A|^2} \frac{k}{E_k} \left\langle \psi_{\mathbf{k}'}^{(+)} \left| W \right| \psi_{\mathbf{k}}^{(+)} \right\rangle \tag{7.60}$$

320   *Scattering Theory of Molecules, Atoms and Nuclei*

is an angle-dependent version of the absorption cross section of Eq. (7.9). The angle refered to here is $\theta = \cos^{-1}\left(\hat{\mathbf{k}}' \cdot \hat{\mathbf{k}}\right)$.

We can define Møller wave operators in the dual space similarly to $\Omega^{(\pm)}$ (see section 4.1). That is, through their action on free states,

$$\Omega^{(\pm)}\left|\phi_{\mathbf{k}}\right\rangle = \left|\psi_{\mathbf{k}}^{(\pm)}\right\rangle \tag{7.61a}$$

$$\tilde{\Omega}^{(\pm)}\left|\phi_{\mathbf{k}}\right\rangle = \left|\tilde{\psi}_{\mathbf{k}}^{(\pm)}\right\rangle. \tag{7.61b}$$

From Eqs. (7.32), (7.33), (7.41) and (7.43), we obtain Lippmann-Schwinger equations

$$\Omega^{(+)}(E_k) = 1 + G_0^{(+)}(E_k)\, V\, \Omega^{(+)}(E_k) = 1 + G^{(+)}(E_k)V \tag{7.62}$$

$$\Omega^{(-)}(E_k) = 1 + G_0^{(-)}(E_k)\, V^\dagger\, \Omega^{(-)}(E_k) = 1 + G_0^{(-)}(E_k)V^\dagger \tag{7.63}$$

$$\tilde{\Omega}^{(+)}(E_k) = 1 + G_0^{(+)}(E_k)\, V^\dagger\, \tilde{\Omega}^{(+)}(E_k) = 1 + \tilde{G}^{(+)}(E_k)V^\dagger \tag{7.64}$$

$$\tilde{\Omega}^{(-)}(E_k) = 1 + G_0^{(-)}(E_k)\, V\, \tilde{\Omega}^{(-)}(E_k) = 1 + \tilde{G}^{(-)}(E_k)V\,. \tag{7.65}$$

The time-dependent representations of these operators are straightforward extensions of Eq. (4.101), as follows

$$\Omega^{(+)} = \lim_{t' \to \infty} e^{-\frac{i}{\hbar}H\left(t'-t\right)}\, e^{\frac{i}{\hbar}H_0\left(t'-t\right)}, \tag{7.66}$$

$$\Omega^{(-)} = \lim_{t' \to -\infty} e^{-\frac{i}{\hbar}H^\dagger\left(t'-t\right)}\, e^{\frac{i}{\hbar}H_0\left(t'-t\right)}, \tag{7.67}$$

$$\tilde{\Omega}^{(+)} = \lim_{t' \to \infty} e^{-\frac{i}{\hbar}H^{\,\dagger}\left(t'-t\right)}\, e^{\frac{i}{\hbar}H_0\left(t'-t\right)}, \tag{7.68}$$

$$\tilde{\Omega}^{(-)} = \lim_{t' \to -\infty} e^{-\frac{i}{\hbar}H\left(t'-t\right)}\, e^{\frac{i}{\hbar}H_0\left(t'-t\right)}. \tag{7.69}$$

7.3 The scattering and the transition operators

In the scattering from a complex potential, the definition of the transition operator, its Lippmann-Schwinger equation and its relation with the scattering amplitude remain the same. That is

$$T = V\,\Omega^{(+)}, \tag{7.70}$$

$$T = V + V G_0^{(+)}T = V + V G^{(+)}V \tag{7.71}$$

$$f(\theta) = -2\pi^2 \left(\frac{2\mu}{\hbar^2}\right) T_{\mathbf{k}',\,\mathbf{k}}, \tag{7.72}$$

with $\theta = \cos^{-1}(\hat{\mathbf{k}}' \cdot \hat{\mathbf{k}})$.

The S-matrix is also given as before (see Eq. (4.79))

$$S_{\mathbf{k}',\mathbf{k}} = \langle \psi_{\mathbf{k}'}^{(-)} | \psi_{\mathbf{k}}^{(+)} \rangle . \tag{7.73}$$

It is easy to prove (problem 1) that the inverse of the S-matrix is given by [Feshbach (1985)]

$$\left(S^{-1} \right)_{\mathbf{k}',\mathbf{k}} = \langle \tilde{\psi}_{\mathbf{k}'}^{(+)} | \tilde{\psi}_{\mathbf{k}}^{(-)} \rangle . \tag{7.74}$$

The fact that the non-hermiticity of the Hamiltonian requires no special care in the evaluation of the scattering amplitude may suggest that a detailed discussion of the dual states is superfluous. However, these states play an important role in some equations involving the T-matrix. An important case is the Distorted-Wave series of Eq. (4.161). Let us consider the two-potential problem (see section 4.5) when V_1 is complex. The Gell-Mann Goldberger formula is still given by

$$T_{\mathbf{k}',\mathbf{k}} = \langle \phi_{\mathbf{k}'} | V_1 | \chi_{\mathbf{k}}^{(+)} \rangle + \langle \chi_{\mathbf{k}'}^{(-)} | V_2 \sum_{m=0}^{\infty} \left(G^{(+)}(E_k) V_2 \right)^m | \chi_{\mathbf{k}}^{(+)} \rangle .$$

However, to write the expansion terms explicitly, we must use the spectral representation of $G^{(+)}$. Since Eq. (4.161) is no longer valid, it must be replaced by Eq. (7.46), which involves the dual states. In this way, Eq. (4.161) becomes

$$\begin{aligned}
T_{\mathbf{k}',\mathbf{k}} = &\langle \chi_{\mathbf{k}'}^{(-)} | V_1 | \phi_{\mathbf{k}} \rangle + \langle \chi_{\mathbf{k}'}^{(-)} | V_2 | \chi_{\mathbf{k}}^{(+)} \rangle \\
&+ \int d^3\mathbf{q} \, \frac{\langle \chi_{\mathbf{k}'}^{(-)} | V_2 | \chi_{\mathbf{q}}^{(+)} \rangle \langle \tilde{\chi}_{\mathbf{q}}^{(+)} | V_2 | \chi_{\mathbf{k}}^{(+)} \rangle}{E_k - E_q \pm i\epsilon} \\
&+ \int d^3\mathbf{q} \, d^3\mathbf{q}' \, \frac{\langle \chi_{\mathbf{k}'}^{(-)} | V_2 | \chi_{\mathbf{q}}^{(+)} \rangle \langle \tilde{\chi}_{\mathbf{q}}^{(+)} | V_2 | \chi_{\mathbf{q}'}^{(+)} \rangle \langle \tilde{\chi}_{\mathbf{q}'}^{(+)} | V_2 | \chi_{\mathbf{k}}^{(+)} \rangle}{(E_k - E_q \pm i\epsilon)(E_k - E_{q'} \pm i\epsilon')} + \cdots .
\end{aligned} \tag{7.75}$$

Note that the DWBA, which consists of keeping only the first line of the above equation, only involves the physical states $|\chi_{\mathbf{k}}^{(+)}\rangle$ and $\langle \chi_{\mathbf{k}'}^{(-)}|$. However, the dual states $\langle \tilde{\chi}_{\mathbf{q}}^{(+)}|$ become essential to evaluate higher order terms in the Distorted Wave series. This is the case of a second order DWBA, which includes the second line of Eq. (7.75).

Further applications of the dual states are encountered in the Low's equation and in the generalized Optical Theorem, discussed below.

322   *Scattering Theory of Molecules, Atoms and Nuclei*

7.3.1   *Low's equation and the generalized Optical Theorem*

We recall from chapter 4 the Low equation (Eq. (4.73)),

$$T_{\mathbf{k}',\mathbf{k}} = V_{\mathbf{k}',\mathbf{k}} + \int d^3\mathbf{q} \, \frac{T_{\mathbf{k}',\mathbf{q}} \, T^*_{\mathbf{k},\mathbf{q}}}{E_k - E_q + i\epsilon} + \sum_n \frac{V_{\mathbf{k}',n} \, V_{n,\mathbf{k}}}{E + B_n} \,, \qquad (7.76)$$

In the case of complex potentials, some modifications are needed. First, we introduce the operator $\tilde{T}$, defined as

$$\tilde{T} = \left(\tilde{\Omega}^{(+)} \right)^\dagger V. \qquad (7.77)$$

Note that $\tilde{T}$ can be considered a generalization of $T^\dagger$, since it reduces to the latter when the imaginary part of V vanishes. Following the same steps as in chapter 4 and neglecting bound states, Low's equation becomes

$$T_{\mathbf{k}',\mathbf{k}} = V_{\mathbf{k}',\mathbf{k}} + \int d^3\mathbf{q} \, \frac{T_{\mathbf{k}',\mathbf{q}} \, \tilde{T}_{\mathbf{k},\mathbf{q}}}{E_k - E_q + i\epsilon} \,, \qquad (7.78)$$

where

$$\tilde{T}_{\mathbf{q},\mathbf{k}} = \tilde{T}^\dagger_{\mathbf{q},\mathbf{k}} = \langle \tilde{\psi}^{(+)}_{\mathbf{q}} | \, V \, | \phi_{\mathbf{k}} \rangle \,. \qquad (7.79)$$

Now we write the analog of Low equation for $\tilde{T}$. The only difference with respect to Eq. (7.76) is the replacement $i\epsilon \to -i\epsilon$. Thus

$$\tilde{T}_{\mathbf{k}',\mathbf{k}} = V_{\mathbf{k}',\mathbf{k}} + \int d^3\mathbf{q} \, \frac{T_{\mathbf{k}',\mathbf{q}} \, \tilde{T}_{\mathbf{k},\mathbf{q}}}{E_k - E_q - i\epsilon} \,. \qquad (7.80)$$

Subtracting Eq. (7.80) from Eq. (7.78), we obtain

$$T_{\mathbf{k}',\mathbf{k}} - \tilde{T}_{\mathbf{k}',\mathbf{k}} = -2\pi i \int d^3\mathbf{q} \, \delta(E_k - E_q) \, T_{\mathbf{k}',\mathbf{q}} \, \tilde{T}_{\mathbf{k},\mathbf{q}} \,. \qquad (7.81)$$

Rewriting Eq. (7.79) in the form

$$\tilde{T}_{\mathbf{q},\mathbf{k}} = \langle \tilde{\psi}^{(+)}_{\mathbf{q}} | \, V^\dagger \, | \phi_{\mathbf{k}} \rangle + \langle \tilde{\psi}^{(+)}_{\mathbf{q}} | \, \left(V - V^\dagger \right) | \phi_{\mathbf{k}} \rangle$$

and using

$$\langle \tilde{\psi}^{(+)}_{\mathbf{q}} | = \langle \psi^{(+)}_{\mathbf{q}} | + \langle \tilde{\psi}^{(+)}_{\mathbf{q}} | \left(V - V^\dagger \right) \frac{1}{E_q - H^\dagger - i\epsilon} \,, \qquad (7.82)$$

which is derived similarly to Eq. (7.55), we get

$$\tilde{T}_{\mathbf{q},\mathbf{k}} = T^\dagger_{\mathbf{q},\mathbf{k}} + \langle \tilde{\psi}^{(+)}_{\mathbf{q}} | \left(V - V^\dagger \right) | \psi^{(-)}_{\mathbf{k}} \rangle \,.$$

Inserting this result into Eq. (7.81), we obtain

$$T_{\mathbf{k}',\mathbf{k}} - T_{\mathbf{k}',\mathbf{k}}^{\dagger} = I_{\mathbf{k}',\mathbf{k}} - 2\pi i \int d^3\mathbf{q}\ \delta(E_k - E_q)\, T_{\mathbf{k},\mathbf{q}} T_{\mathbf{q},\mathbf{k}'}^{\dagger}\,, \qquad (7.83)$$

where $I_{\mathbf{k}',\mathbf{k}}$ stands for

$$
\begin{aligned}
I_{\mathbf{k}',\mathbf{k}} = {}& \langle \tilde{\psi}_{\mathbf{k}'}^{(+)} |\ \left(V - V^{\dagger}\right) |\psi_{\mathbf{k}}^{(-)}\rangle \\
& - 2\pi i \int d^3\mathbf{q}\ \delta(E_k - E_q)\, T_{\mathbf{k},\mathbf{q}}\ \langle \tilde{\psi}_{\mathbf{q}}^{(+)} |\ \left(V - V^{\dagger}\right) |\psi_{\mathbf{k}}^{(-)}\rangle\,,
\end{aligned}
$$

or

$$I_{\mathbf{k}',\mathbf{k}} = \int d^3\mathbf{q}\ [\delta(\mathbf{k} - \mathbf{q}) - 2\pi i\, \delta(E_k - E_q)\, T_{\mathbf{k},\mathbf{q}}]\ \langle \tilde{\psi}_{\mathbf{q}}^{(+)} |\ \left(V - V^{\dagger}\right) |\psi_{\mathbf{k}}^{(-)}\rangle\,.$$
$$(7.84)$$

Now we replace (see Eqs. (4.82) and (4.79))

$$\delta(\mathbf{k} - \mathbf{q}) - 2\pi i\, \delta(E_k - E_q)\, T_{\mathbf{k},\mathbf{q}} = S_{\mathbf{k},\mathbf{q}} = \left\langle \psi_{\mathbf{k}}^{(-)} \big| \psi_{\mathbf{q}}^{(+)} \right\rangle$$

and move $\left\langle \psi_{\mathbf{k}}^{(-)} \right|$ out of the integral over $\mathbf{q}$. Eq. (7.84) then becomes

$$I_{\mathbf{k}',\mathbf{k}} = \left\langle \psi_{\mathbf{k}}^{(-)} \right|\ \left[\int |\psi_{\mathbf{q}}^{(+)}\rangle\, d^3\mathbf{q}\ \left\langle \tilde{\psi}_{\mathbf{q}}^{(+)} \right| \right]\ \left(V - V^{\dagger}\right) |\psi_{\mathbf{k}}^{(-)}\rangle, \qquad (7.85)$$

or (see Eq. (7.38)),

$$I_{\mathbf{k}',\mathbf{k}} = \langle \psi_{\mathbf{k}}^{(-)} |\ \left(V - V^{\dagger}\right) |\psi_{\mathbf{k}}^{(-)}\rangle. \qquad (7.86)$$

Next, we take into account Eq. (7.58) to write $I_{\mathbf{k}',\mathbf{k}}$ as

$$I_{\mathbf{k}',\mathbf{k}} = - \langle \psi_{\mathbf{k}}^{(+)} |\ \left(V - V^{\dagger}\right) |\psi_{\mathbf{k}}^{(+)}\rangle, \qquad (7.87)$$

and insert this result into Eq. (7.83). We obtain

$$T_{\mathbf{k}',\mathbf{k}} - T_{\mathbf{k}',\mathbf{k}}^{\dagger} = - \langle \psi_{\mathbf{k}}^{(+)} |\ \left(V - V^{\dagger}\right) |\psi_{\mathbf{k}}^{(+)}\rangle - 2\pi i \int d^3\mathbf{q}\ \delta(E_k - E_q)\, T_{\mathbf{k},\mathbf{q}} T_{\mathbf{q},\mathbf{k}'}^{\dagger},$$
$$(7.88)$$

or, using Eq. (7.60)

$$T_{\mathbf{k}',\mathbf{k}} - T_{\mathbf{k}',\mathbf{k}}^{\dagger} = -2\pi i \int d^3\mathbf{q}\ \delta(E_k - E_q)\, T_{\mathbf{k},\mathbf{q}} T_{\mathbf{q},\mathbf{k}'}^{\dagger}\ + 2i\frac{E}{k}\, \Sigma_{\mathbf{k}',\mathbf{k}}^{a}\,. \qquad (7.89)$$

For $\mathbf{k}' = \mathbf{k}$, the above equation can be cast in the form of the generalized optical theorem, Eq. (7.24), since

$$\Sigma_{\mathbf{k},\mathbf{k}}^{a} = \sigma_a\,.$$

Scattering Theory of Molecules, Atoms and Nuclei

When the Hamiltonian has an absorptive term, the S-matrix is not unitary. Eq. (7.89) can be used to construct the unitarity defect operator, defined as

$$\Delta = \mathbf{1} - SS^\dagger \,, \tag{7.90}$$

where $\mathbf{1}$ stands for the identity operator. Employing the relation between the S- and the T-matrices (Eq. (4.82)), which remains valid for complex potentials, and using Eq. (7.89), one easily finds

$$\Delta_{\mathbf{k}'\mathbf{k}} = -4\pi\, \delta\left(E_{k'} - E_k\right) \frac{E_k}{k}\ \Sigma^a_{\mathbf{k}'\mathbf{k}}. \tag{7.91}$$

7.4   Partial-wave expansions

In the following we derive the quantities that are modified by absorption (complexity of the potential). In particular, we check how the partial-wave expansions are affected. We mention at the outset that, formally, the complex nature of the interaction requires the introduction of the scattering wave functions discussed in section 7.2. However, in so far as the calculation of the T and S operators and their matrix elements are concerned, only the physical scattering states $|\psi_{\mathbf{k}}^{(+)}\rangle$ and $|\psi_{\mathbf{k}}^{(-)}\rangle$, defined in Eqs.(7.32) and (7.33), enter. It can easily be checked that the procedures of section 2.3 can still be followed, so that the partial-wave expansion of $\psi_{\mathbf{k}}^{(+)}(\mathbf{r})$ is given by Eq. (2.57a) with $A = (2\pi)^{-3/2}$. That is,

$$\psi_{\mathbf{k}}^{(+)}(\mathbf{r}) = \frac{1}{(2\pi)^{3/2}} \sum_{lm} 4\pi\, Y_{lm}^*(\hat{\mathbf{k}})\, Y_{lm}(\hat{\mathbf{r}})\, i^l\, \frac{u_l(k,r)}{kr}\,. \tag{7.92}$$

However, the phase shifts contained in the radial wave function are now complex. The partial-wave expansion of the ingoing solution, which is obtained through the time-reversal operation, $\psi_{\mathbf{k}}^{(-)}(\mathbf{r}) = \left(\psi_{-\mathbf{k}}^{(+)}(\mathbf{r})\right)^*$ (see section 4.6), is

$$\psi_{\mathbf{k}}^{(-)}(\mathbf{r}) = \frac{1}{(2\pi)^{3/2}} \sum_{lm} 4\pi\, Y_{lm}^*(\hat{\mathbf{k}})\, Y_{lm}(\hat{\mathbf{r}})\, i^l\, \frac{u_l^*(k,r)}{kr} \tag{7.93}$$

The corresponding dual wave functions can be expanded as

$$\tilde{\psi}_{\mathbf{k}}^{(+)}(\mathbf{r}) = \frac{1}{(2\pi)^{3/2}} \sum_{lm} 4\pi\, Y_{lm}^*(\hat{\mathbf{k}})\, Y_{lm}(\hat{\mathbf{r}})\, i^l\, \frac{\tilde{u}_l(k,r)}{kr} \tag{7.94}$$

$$\tilde{\psi}_{\mathbf{k}}^{(-)}(\mathbf{r}) = \frac{1}{(2\pi)^{3/2}} \sum_{lm} 4\pi\, Y_{lm}^*(\hat{\mathbf{k}})\, Y_{lm}(\hat{\mathbf{r}})\, i^l\, \frac{\tilde{u}_l^*(k,r)}{kr}\,. \tag{7.95}$$

The wave functions $u_l(k,r)$ and $\tilde{u}_l(k,r)$ are respectively the solutions of the radial equations with the Hamiltonians H and $H^\dagger$, with the boundary condition of an outgoing scattered wave. At asymptotic distances they are

$$u_l(k, r \to \infty) = \frac{i}{2} \left[e^{-i(kr - l\pi/2)} - S_l \, e^{i(kr - l\pi/2)} \right] \tag{7.96}$$

$$\tilde{u}_l(k, r \to \infty) = \frac{i}{2} \left[e^{-i(kr - l\pi/2)} - \tilde{S}_l \, e^{i(kr - l\pi/2)} \right]. \tag{7.97}$$

Above, S_l is the partial-wave component of the S-matrix in the scattering from the potential[4] $V = U - iW$ while $\tilde{S}_l$ is that in the scattering from the potential $V^\dagger = U + iW$. Since $-iW$ is a sink of flux, one must have $|S_l| \equiv |e^{2i\delta_l}| < 1$. On the other hand, $+iW$ acts as a source and therefore $|\tilde{S}_l| \equiv |e^{2i\tilde{\delta}_l}| > 1$. The orthonormality relation involving u_l and $\tilde{u}_l$ is a straightforward extension of Eq. (4.173) to complex potentials. Inserting the partial-wave expansions of Eqs. (7.92) and (7.94) into Eq. (7.36), we obtain

$$\int_0^\infty dr \; \tilde{u}_l^*(k, r) \, u_l(k', r) = \frac{\pi}{2} \, \delta(k - k'). \tag{7.98}$$

The operators S and $\tilde{S}$ can also be expressed in terms of their partial-wave components. Proceeding as in chapter 4, we write

$$S_{\mathbf{k}', \mathbf{k}} = \delta(E_{k'} - E_k) \, \frac{\hbar^2}{\mu k} \sum_{lm} Y_{lm}(\hat{\mathbf{k}}') Y_{lm}^*(\hat{\mathbf{k}}) \, S_l(E_k) \tag{7.99}$$

and

$$\tilde{S}_{\mathbf{k}', \mathbf{k}} = \delta(E_{k'} - E_k) \, \frac{\hbar^2}{\mu k} \sum_{lm} Y_{lm}(\hat{\mathbf{k}}') Y_{lm}^*(\hat{\mathbf{k}}) \, \tilde{S}_l(E_k). \tag{7.100}$$

It is straightforward to show that (see exercise 6.2)

$$\tilde{S}_l = \frac{1}{S_l^*}. \tag{7.101}$$

Thus, the phase of $\tilde{S}_l$ is identical to that of S_l while its modulus is

$$\left| \tilde{S}_l \right| = \frac{1}{|S_l|}. \tag{7.102}$$

The wave-functions $\tilde{u}_l(k,r)$ and $u_l(k,r)$ are connected through the expression

---

[4]From this point, we use a different notation for the imaginary potential. To emphasize its absorptive nature, we write $V = U - iW$, where W is a positive function. In section 7.1 we wrote (see Eq. (7.2)) $V = U + iW$ with W standing for a negative function. Both notations are commonly found in the literature.

$$\tilde{u}_l(k,r) = u_l^*(k,r) \; \tilde{S}_l. \tag{7.103}$$

The validity of Eq. (7.103) at asymptotic distances can be trivially confirmed. Taking the conjugate of Eq. (7.96), replacing $\delta_l^* = \tilde{\delta}_l$ and comparing with Eq. (7.97) we get the above result. The generalization to any r requires more work.   Using the partial-wave expansions of Eqs. (7.92) and (7.93) in Eq. (7.73) and comparing the result with the partial-wave expansion of the S-matrix (Eq. (7.99)) we get

$$\int_0^\infty dr \; u_l(k,r) \, u_l(k',r) = \frac{\pi}{2} \; S_l \; \delta(k-k'). \tag{7.104}$$

In the derivation of the above equation, the relation

$$\delta(E_k - E_{k'}) = \frac{\mu}{k\hbar^2} \, \delta(k-k')$$

was used. To prove Eq. (7.103), we must show that it satisfies the orthonormality relation that defines the dual states. That is,

$$\int_0^\infty dr \; \left[u_l^*(k,r) \; \tilde{S}_l \right]^* \, u_l(k',r) = \frac{\pi}{2} \, \delta(k-k') \, .$$

Calling

$$X = \int_0^\infty dr \; \left[u_l^*(k,r) \; \tilde{S}_l \right]^* \, u_l(k',r)$$

$$= \frac{1}{S_l} \; \int_0^\infty dr \; u_l(k,r) \; u_l(k',r)$$

and replacing the above radial integral by the result of Eq. (7.104), we get the desired proof.

7.5   Diffractive scattering

In this section we use the semiclassical approximation for the scattering amplitude (see section 5.2.3) to discuss the diffractive nature of the scattering from complex potentials. We start with the semiclassical expression of the scattering amplitude of Eq. (5.268),

$$f(\theta) = \frac{1}{ik} \int_0^\infty d\lambda \, \lambda \; [S(\lambda) - 1] \; P_\lambda(\cos\theta), \tag{7.105}$$

and the cross section

$$\frac{d\sigma(\theta)}{d\Omega} = |f(\theta)|^2 \, .$$

The above integral can easily be evaluated in the limiting case of strong absorption where the modulus of the *l*-components of the S-matrix can be approximated by the *sharp cut-off* absorption,

$$\left|S(\lambda)\right| = 0 \qquad \text{for} \qquad \lambda < \bar{\Lambda},$$
$$= 1 \qquad \text{for} \qquad \lambda \geq \bar{\Lambda}.$$

The cut-off angular momentum is given by $\bar{\Lambda} = k\bar{R}$, with $\bar{R}$ being the characteristic radius of the scatterer. There are two types of known diffraction scenarios borrowed from Physical Optics:

(1) *Fraunhofer diffraction* - characterized by pure black-disk absorption (no refraction associated with a real phase shift). It corresponds to the diffraction of a beam of parallel rays of light emitted by a source at an infinite distance from the disc.

(2) *Fresnel diffraction* - characterized by black-disc absorption but with real Coulomb phase shift, which renders the source of the rays to be at a finite distance from the disk. It corresponds to the diffraction of light from a source located near the scatterer.

Both cases are based on the guiding optical properties of Babinet principle, which states that the scattering from a disc is equivalent to that from an aperture with the same radius. In the following we describe the scattering in these limiting cases, which represent the qualitative effects of absorptive interactions (more details can be find in [Hussein and McVoy (1984); Nussenzveig (1992); Frahn (1985)]).

7.5.1   *Fraunhofer diffraction*

In this case one neglects any refractive effect, setting $\delta(\lambda) = 0$. The S-matrix can then be written

$$S(\lambda) \equiv \left|S(\lambda)\right| e^{2i\delta(\lambda)} \simeq \left|S(\lambda)\right|. \tag{7.106}$$

Simple analytical results can be obtained if one adopts the sharp cut-off approximation,

$$S(\lambda) = 0, \qquad \text{for } \lambda < \bar{\Lambda},$$
$$= 1, \qquad \text{for } \lambda \geq \bar{\Lambda}. \tag{7.107}$$

Above, $\bar{\Lambda}$ represents the angular momentum for a grazing collision, which is given in terms of the radius of the scatterer, $\bar{R}$, and wave number, k, by the relation, $\bar{\Lambda} = k\bar{R}$.

328   *Scattering Theory of Molecules, Atoms and Nuclei*

In typical situations Franhofer diffraction occurs at small scattering angles. Thus, one can adopt the asymptotic (large λ) approximation of Eq. (5.381),

$$P_\lambda(\cos\theta) \to \left(\frac{\theta}{\sin\theta}\right)^{1/2} J_0(\lambda\theta). \tag{7.108}$$

Using Eqs. (7.107) and (7.108), the scattering amplitude of Eq. (7.105) becomes

$$f(\theta) = \frac{1}{ik} \left(\frac{\theta}{\sin\theta}\right)^{1/2} \int_0^\infty d\lambda \; (\,|S(\lambda)| - 1)\; [\lambda\, J_0(\lambda\theta)], \tag{7.109}$$

or, changing variable: $\lambda \to x = \lambda\theta$,

$$f(\theta) = \frac{1}{ik\theta^2} \left(\frac{\theta}{\sin\theta}\right)^{1/2} \int_0^\infty dx \; (\,|S(x/\theta)| - 1)\; [x\, J_0(x)]. \tag{7.110}$$

The above integral can be evaluated by parts. Using the result[5]

$$\frac{d}{dx}[xJ_1(x)] = xJ_0(x), \tag{7.111}$$

where J_0 and J_1 are respectively the cylindrical Bessel functions of order 0 and 1, and having in mind that

$$\left[x\,J_1(x)\,\big(\,|S(x/\theta)| - 1\big)\right]_0^\infty = 0,$$

we get

$$f(\theta) = \frac{i}{k\theta^2} \left(\frac{\theta}{\sin\theta}\right)^{1/2} \int_0^\infty dx \; [x\, J_1(x)] \; \frac{d}{dx}|S(x/\theta)|. \tag{7.112}$$

Within the sharp cut-off approximation for the S-matrix, we can write[6],

$$|S(x/\theta)| = \Theta(x - \bar{X}) \;\longrightarrow\; \frac{d}{dx}\left(|S(x/\theta)| - 1\right) = \delta(x - \bar{X}), \tag{7.113}$$

and $f(\theta)$ becomes

$$f(\theta) = \frac{i\bar\Lambda}{k} \left(\frac{\theta}{\sin\theta}\right)^{1/2} \left[\frac{J_1(\bar\Lambda\theta)}{\theta}\right] = i\bar{R} \left(\frac{\theta}{\sin\theta}\right)^{1/2} \left[\frac{J_1(\bar\Lambda\theta)}{\theta}\right]. \tag{7.114}$$

---

[5]This can easily be obtained using the ascending series for the Bessel functions [Abramowitz and Stegun (1972)].

[6]In this sub-section, we use the standard notations Θ and δ for the step-function and the Dirac delta function, respectively. They should not be confused with the classical deflection function and the phase shifts, which are represented by these symbols in other sections of this book.

The cross section for Fraunhofer scattering, given by $\left|f(\theta)\right|^2$, is

$$\frac{d\sigma(\theta)}{d\Omega} = \bar{R}^2 \left(\frac{\theta}{\sin\theta}\right) \left[\frac{J_1(\bar{\Lambda}\theta)}{\theta}\right]^2. \qquad (7.115)$$

For small angles, $\sin\theta/\theta \approx 1$ and the cross section reduces to

$$\frac{d\sigma(\theta)}{d\Omega} = \bar{R}^2 \left[\frac{J_1(\bar{\Lambda}\theta)}{\theta}\right]^2. \qquad (7.116)$$

For large values of $\bar{\Lambda}$ and not too small θ, $x = \bar{\Lambda}\theta \gg 1$ and one can use the asymptotic expression for cylindrical Bessel functions [Watson (1966)]

$$J_m(x) \simeq \sqrt{\frac{2}{\pi x}} \, \cos\left(x - m\pi/2 - \pi/4\right). \qquad (7.117)$$

The scattering amplitude then becomes

$$f(\theta) = \frac{i\bar{R}}{\theta} \left(\frac{1}{\bar{\Lambda}\pi\sin\theta}\right)^{1/2} \left[\sin(\bar{\Lambda}\theta) - \cos(\bar{\Lambda}\theta)\right] \qquad (7.118)$$

and the corresponding cross section is

$$\frac{d\sigma(\theta)}{d\Omega} = \bar{R}^2 \left[\frac{1 - \sin\left(2\bar{\Lambda}\theta\right)}{\pi\,\bar{\Lambda}\theta^2\sin\theta}\right]. \qquad (7.119)$$

In figure 7.1 we show the cross sections for Fraunhofer scattering given by Eq. (7.115) (solid line) and by the approximate expression of Eq. (7.119) (dashed line). The cross sections are shown both in linear (top panel) and logarithmic (bottom panel) scales. The two curves are quite close for angles $\theta \gtrsim \theta_0 = 5^\circ$. This corresponds to $x \gtrsim \theta_0\,\bar{\Lambda} \times \pi/180 \simeq 4.4$, where the approximation of Eq. (7.117) is accurate. At angles below θ_0, the two curves are very different. The approximate curve is out of phase and diverges at $\theta = 0$.

To discuss the period of oscillation, it is convenient to re-write Eq. (7.116) as

$$\frac{d\sigma(\theta)}{d\Omega} = \left(\bar{\Lambda}R\right)^2 \left[\frac{J_1(x)}{x}\right]^2. \qquad (7.120)$$

The period corresponds to the difference between the x-values where $J_1(x)/x$ reaches the first two consecutive maxima. The first is clearly at $x_1 = 0$. The second, determined through numerical calculation of the
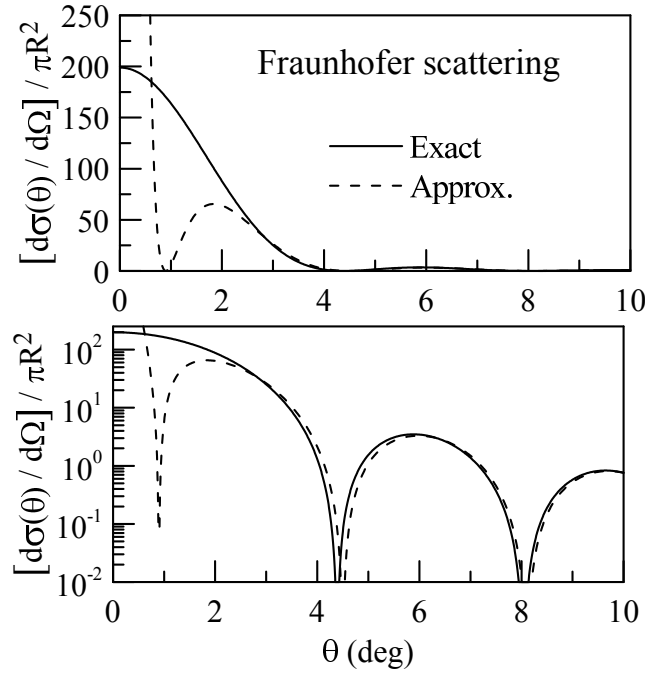
Fig. 7.1   Fraunhofer scattering cross sections normalized with respect to the geometrical cross section, shown in linear (top panel) and logarithmic (bottom panel) scales. The semiclassical calculations were made with a sharp cut-off S-matrix, with $\bar{\Lambda} = 50$. The solid and the dashed lines correspond respectively to the results obtained with the semiclassical expression of Eq. (7.115) and with its approximate version (Eq. (7.119)).

$J_1(x)/x$ ratio, is $x_2 = 5.1$. Thus, we can write, $\Delta x = x_2 - x_1 = 5.1$. The corresponding angular period is

$$\Delta\theta^o = \frac{x_2}{\bar{\Lambda}} \times \frac{180}{\pi} = 5.8^o. \qquad (7.121)$$

It is interesting to check the concentration of the Fraunhofer cross section at the forward direction. Similarly to the case of forward glory, we can measure this concentration through the ratio of the cross sections at the first two consecutive maxima. The *forward concentration parameter* for Fraunhofer scattering, α_{F}, then is

$$\alpha_{\mathrm{F}} = \lim_{x_1 \to 0} \left[\frac{x_2 \, J_1(x_1)}{x_1 \, J_1(x_2)} \right]^2 = 57. \qquad (7.122)$$

As in the case of forward glory, the above parameter is a general characteristic of Fraunhofer scattering. It does not depend on the collision energy or any property of the system. The only requirement is that the modulus of the S-matrix can be approximated by a sharp cut-off.

The forward angle concentration in Fraunhofer scattering is much more pronounced than that in glory scattering [Nussenzveig (1992)]. The concentration parameter for the former is almost one order of magnitude larger than the one for the latter ($\alpha_g = 6.2$). This may be a practical mean to distinguish the nature of observed cross sections. Frauhofer scattering and glory arise from very different physical processes. The former is a diffractive effect associated with the imaginary part of the optical potential, whereas the latter is a refractive effect, related with the real part of the potential. However, the period of oscillation for the two processes can be rather similar. Furthermore, it depends on some angular momentum that may be model dependent. In this way, the ratio of the cross sections at the first two consecutive maxima gives a better indication of the physics involved.

The sharp-cutoff limit is seldom really attained, except in light scattering from water droplets [Nussenzveig (1992)]. Most physical systems have diffused absorption surfaces. In such cases, the modulus of the partial-wave projected S-matrix can be expressed in terms of two parameters: the cut-off parameter, $\bar{\Lambda}$, and a diffuseness parameter, Δ. In the *smooth cut-off* model (SCO), $|S(\lambda)|$ is approximated by some simple function of λ, depending on these two parameters. As we will show, the diffuseness of the absorptive potential brings in more damping in the angular oscillation. We discuss below a simple implementation of the smooth cut-off model.

As a starting point, we rewrite Eq. (7.112) as

$$
f(\theta) = \frac{i}{k\theta} \left(\frac{\theta}{\sin\theta} \right)^{1/2} \int_{-\infty}^{\infty} d\lambda \ [\lambda \, J_1(\lambda\theta)] \ \frac{d}{d\lambda} |S(\lambda)|. \tag{7.123}
$$

Note that in the above equation we have extended the lower limit of the integral to $-\infty$. This limit originally was zero. Since $\Delta \ll \bar{\Lambda}$, the integrand at $\lambda \le 0$ is vanishingly small and thus the modification of the lower limit has no practical consequence.

In the smooth cut-off model, the derivative of $|S(\lambda)|$ is no longer a delta function. However, it is sharply peaked at $\lambda = \bar{\Lambda}$ and the width of the peak is measured by the parameter Δ ($\Delta \ll \bar{\Lambda}$). We use the notation

$$D_\Delta(\lambda - \bar\Lambda) = \frac{d}{d\lambda} \big| S(\lambda) \big|, \tag{7.124}$$

and point out that this function has the limit

$$\lim_{\Delta \to 0} \big[D_\Delta(\lambda - \bar\Lambda) \big] = \delta(\lambda - \bar\Lambda). \tag{7.125}$$

Now we use the asymptotic form[7] of the cylindrical Bessel functions (Eq. (7.117)) for $m = 1$,

$$J_1(x) \simeq \sqrt{\frac{2}{\pi x}} \, \cos(x - \pi/2 - \pi/4) \equiv \sqrt{\frac{2}{\pi x}} \, \sin(x - \pi/4). \tag{7.126}$$

Inserting this result into Eq. (7.123) and neglecting the variation of $\sqrt{\lambda}$ within the range of $D_\Delta(\lambda - \bar\Lambda)$, we get

$$f_\Delta(\theta) = \frac{1}{k\theta} \left(\frac{\bar\Lambda}{2\pi \sin\theta} \right)^{1/2} \left[I_\Delta^{(+)}(\theta) \, e^{i(\bar\Lambda\theta - \pi/4)} - I_\Delta^{(-)}(\theta) \, e^{-i(\bar\Lambda\theta - \pi/4)} \right]. \tag{7.127}$$

Above, we have introduced the diffraction damping functions

$$I_\Delta^{(\pm)}(\theta) = \int_{-\infty}^{\infty} d\lambda \, D_\Delta(\lambda - \bar\Lambda) \, e^{\pm i(\lambda - \bar\Lambda)\,\theta}$$

$$= \int_{-\infty}^{\infty} dz \, D_\Delta(z) \, e^{\pm i\, z\theta}. \tag{7.128}$$

Note that we have changed variable $\lambda \to z = \lambda - \bar\Lambda$.

Closed expressions for the scattering amplitude can be obtained if one adopts convenient parametrizations for the modulus of the S-matrix. We consider here the choice

$$\big| S(\lambda) \big| = \frac{1}{1 + \exp\left[(\bar\Lambda - \lambda)/\Delta \right]}, \tag{7.129}$$

which reduces to the sharp cut-off approximation in the $\Delta \to 0$ limit. In this case, one immediately obtains

$$D_\Delta(z) = \frac{e^{z/\Delta}}{\Delta \left[1 + e^{z/\Delta} \right]^2}, \tag{7.130}$$

---

[7]In principle, the use of the asymptotic form of the Bessel function would imply that the resulting scattering amplitude is not valid at small scattering angles. However, it is not so. The same results can be obtained writing the Legendre polynomials in terms of traveling waves components, $Q_l^{(\pm)}(x)$, like in Fuller's near-side decomposition [Fuller (1975a); Brink (1985)], instead of $J_1(x)$. The asymptotic forms would then enter only in the evaluation of the integrals in the complex plane over an asymptotic contour, which appear later in this section.

and the integrals of Eq. (7.128) become

$$I_\Delta^{(\pm)}(\theta) = \frac{1}{\Delta} \int_{-\infty}^{\infty} dz \; \frac{e^{z/\Delta}}{\left[1 + e^{z/\Delta}\right]^2} \; e^{\pm i\,z\theta}. \qquad (7.131)$$

These integrals can be calculated taking closed contours in the complex plane. The integrands have double poles at the points

$$z_n = i\pi \, (2n + 1) \, \Delta. \qquad (7.132)$$

The evaluation of the diffraction damping functions can be performed using the residue theorem for double poles and taking only the leading pole ($n = 0$) into account. One gets

$$I_\Delta^{(+)}(\theta) = I_\Delta^{(-)}(\theta) \equiv I_\Delta(\theta) = \frac{\pi\theta\Delta}{\sin(\pi\theta\Delta)}. \qquad (7.133)$$

Now one inserts this result into Eq. (7.127) and move $I_\Delta(\theta)$ out of the square brackets. One is left with $2i\sin(\bar\Lambda\theta - \pi/4)$, which can be expressed in terms of $J_1(\bar\Lambda\theta)$ (see Eq. (7.126)). In this way, the smooth cut-off scattering amplitude can be put in the form

$$f_\Delta(\theta) = f_{\rm sco}(\theta) \times I_\Delta(\theta), \qquad (7.134)$$

and the cross section becomes

$$\frac{d\sigma_\Delta(\theta)}{d\Omega} = \frac{d\sigma_{\rm sco}(\theta)}{d\Omega} \times I_\Delta^2(\theta). \qquad (7.135)$$

In the above equations, $f_{\rm sco}(\theta)$ is the scattering amplitude within the sharp cut-off approximation, given in Eq. (7.114), and $d\sigma_{\rm sco}(\theta)/d\Omega$ is the corresponding cross section (Eq. (7.115)).

An example of the damping produced by smooth cut-off absorption is given in figure 7.2. The system is the same of figure 7.1 and the sharp cut-off cross section is still represented by a solid line. The dashed line corresponds to smooth cut-off absorption, with $|S(\lambda)|$ given by Eq. (7.129), with $\Delta = 5$ units of angular momentum. This corresponds to 10% of the grazing angular momentum, $\bar\Lambda = 50$. One notices that the smooth cut-off absorption leads to a stronger concentration of the cross section in the forward region. In this case, the forward concentration parameter of Eq. (7.122) is considerably larger then for sharp cut-off ($\alpha_{\rm F} = 57$), reaching the value

$$\alpha_{\rm F}(\Delta = 5) = 125. \qquad (7.136)$$

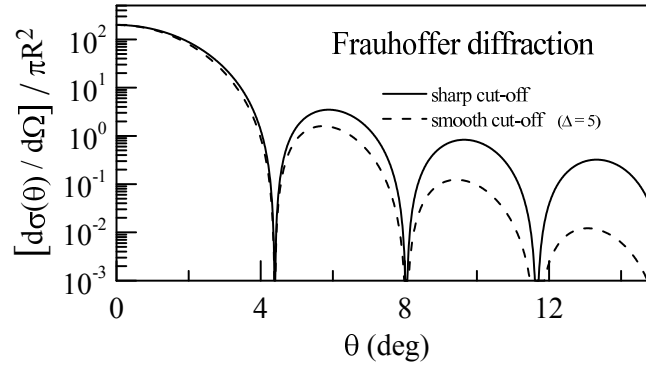334   *Scattering Theory of Molecules, Atoms and Nuclei*

Fig. 7.2   Comparison between the semiclassical cross sections obtained with the sharp-cutt-off (solid line) and the smooth-cut-off (dashed line) approximations. In the latter, we used $\Delta = 5$. As in the previous figure, the cross sections are normalized with respect to the geometric value.

7.5.2   *Fresnel diffraction*

We now consider the effect of a strong Coulomb field on the diffraction pattern. It is expected to introduce refractive effects in the near-side (Coulomb repulsion) or in the far-side (Coulomb attraction) scattering amplitude. We concentrate here on the Fresnel diffraction associated with the near-side amplitude and to simplify the notation we omit the superscript $(-)$ in the near-side branch of the scattering amplitude.

The starting point is the semiclassical expression for the near-side amplitude of Eq. (5.274), using the the sharp cut-off approximation for the modulus of the S-matrix and Coulomb phase shifts for its phase,

$$S(\lambda) = 0, \qquad \text{for } \lambda \leq \bar{\Lambda}$$
$$= e^{2i\sigma(\lambda)}, \qquad \text{for } \lambda > \bar{\Lambda}. \qquad (7.137)$$

In this case, the scattering amplitude can be written as

$$f(\theta) = \frac{e^{-i\pi/4}}{k} \left(\frac{1}{2\pi \sin\theta} \right)^{1/2} \int_{\bar{\Lambda}}^{\infty} d\lambda \, \lambda^{1/2} \, e^{i\,[2\sigma(\lambda) - \lambda\theta]}. \qquad (7.138)$$

Before we evaluate the above integral, it is convenient to consider the pure Coulomb amplitude (no absorption), which is given by Eq. (5.274) with the S-matrix

$$S(\lambda) = e^{2i\sigma(\lambda)}. \qquad (7.139)$$

That is[8]

$$f_{\mathrm{C}}(\theta) = \frac{e^{-i\pi/4}}{k} \left(\frac{1}{2\pi \sin \theta}\right)^{1/2} \int_0^\infty d\lambda \; \lambda^{1/2} \; e^{i\,[2\sigma(\lambda) - \lambda\theta]}. \qquad (7.140)$$

Note that the only difference between the above semiclassical Coulomb amplitude and the sharp cut-off scattering amplitude of Eq. (7.138) is the lower limit of integration. Above, this limit is zero whereas in Eq. (7.138) it is the grazing angular momentum $\bar{\Lambda}$.

The integrals of Eqs. (7.138) and (7.140) can be evaluated by the stationary phase approximation. The stationary phase occurs at the angular momentum λ_0 where the phase of the integrand,

$$\varphi(\lambda) \equiv 2\sigma(\lambda) - \lambda\theta, \qquad (7.141)$$

satisfies the condition

$$\left[\frac{d\varphi(\lambda)}{d\lambda}\right]_{\lambda=\lambda_0} = \left[\frac{d}{d\lambda}\left(2\sigma(\lambda) - \lambda\theta\right)\right]_{\lambda=\lambda_0} = 0. \qquad (7.142)$$

Since $d[2\sigma(\lambda)]/d\lambda$ is the classical deflection function for the Coulomb potential, this condition can be written

$$\Theta(\lambda_0) = \theta. \qquad (7.143)$$

Using the above equation in the relation between the Coulomb deflection function and the angular momentum (Eq. (3.11c)), one gets an analytical expression for λ_0 in terms of the observation angle, θ, and the Sommerfeld parameter, η,

$$\lambda_0 = \frac{\eta}{\tan \theta/2}. \qquad (7.144)$$

Next, we expand $\varphi(\lambda)$ around λ_0 and keep terms up to second order. Owing to the stationary phase condition, the term of first order vanishes and the truncated expansion gives

$$\varphi(\lambda) \simeq \varphi_0 + \frac{\Theta_0'}{2}\,(\lambda - \lambda_0)^2. \qquad (7.145)$$

Above, we used the short-hand notations: $\varphi_0 \equiv \varphi(\lambda_0)$ and $\Theta_0' \equiv \Theta'(\lambda_0)$.

---

[8]Although the Coulomb amplitude cannot be calculated by a truncated summation of the partial-wave series, the integral introduced in the semiclassical approximation can be evaluated with the upper limit going to infinity. As it will be shown below, the semiclassical approximation to the Coulomb scattering amplitude leads to the correct cross section.

336   *Scattering Theory of Molecules, Atoms and Nuclei*

In typical situations, $\lambda_0 \gg 0$, except for very backward angles, which are not important in the study of Fresnel diffraction. The lower limit of the integrals can then be extended to $-\infty$, without affecting the values of the scattering amplitude. Adopting this procedure and approximating $\lambda^{1/2} \simeq \lambda_0^{1/2}$, Eq. (7.138) becomes

$$f_{\rm C}(\theta) = \frac{e^{i\varphi_0 - i\pi/4}}{k} \left(\frac{\lambda_0}{2\pi \sin\theta} \right)^{1/2} \int_{-\infty}^{\infty} d\lambda \, e^{i\Theta_0' \, (\lambda - \lambda_0)^2/2}. \tag{7.146}$$

Using the explicit form of λ_0 (Eq. (7.144)) and the relation $\sin\theta = 2\sin\theta/2 \cos\theta/2$, the scattering amplitude takes the form

$$f_{\rm C}(\theta) = \frac{e^{i\varphi_0 - i\pi/4}}{2k \sin\theta/2} \left(\frac{\eta}{\pi} \right)^{1/2} \int_{-\infty}^{\infty} d\lambda \, e^{i\Theta_0' \, (\lambda - \lambda_0)^2/2} \,. \tag{7.147}$$

To evaluate the above integral, we change to a new variable t such that

$$i\frac{\Theta_0'}{2} (\lambda - \lambda_0)^2 \longrightarrow -t^2. \tag{7.148}$$

This is achieved by the transformation[9]

$$t = e^{i\pi/4} \left(\frac{-\Theta_0'}{2} \right)^{1/2} (\lambda - \lambda_0) \,, \tag{7.149}$$

which leads to the relation

$$d\lambda = e^{-i\pi/4} \left(\frac{2}{-\Theta_0'} \right)^{1/2} dt. \tag{7.150}$$

Inserting Eqs. (7.149) and (7.150) into Eq. (7.147) and using the value of the gaussian integral,

$$\int_{-\infty}^{\infty} dt \, e^{-t^2} = \sqrt{\pi}, \tag{7.151}$$

we get

$$f_{\rm C}(\theta) = \frac{e^{i\varphi_0 - i\pi/2}}{2k \sin\theta/2} \left(\frac{2\eta}{-\Theta_0'} \right)^{1/2} \,. \tag{7.152}$$

The derivative of the deflection function appearing above, which can be obtained through direct differentiation of Eq. (3.11c) , is

$$\Theta_0' = -\frac{2}{\eta} \sin^2(\theta/2) \,. \tag{7.153}$$

---

[9]It is convenient to keep the minus sign together with Θ_0' to cancel the minus sign contained in the derivative of the Coulomb deflection function.

Inserting this result into Eq. (7.162), one obtains the semiclassical approximation for the Coulomb amplitude

$$f_{\rm C}(\theta) = \frac{a}{2 \sin^2 \theta/2} \; e^{i[2\sigma(\lambda_0) - \lambda_0\theta - \pi/2]} \; , \qquad (7.154)$$

where $a = \eta/k$ is the half-distance of closest approach in a head-on collision, discussed in chapter 3. The semiclassical Coulomb cross section then is

$$\frac{d\sigma_{\rm C}(\theta)}{d\Omega} = \frac{a^2}{4} \left[\frac{1}{\sin^4 \theta/2} \right]. \qquad (7.155)$$

Note that the semiclassical approximation leads to the correct cross section of Eq. (3.35). The phase of the semiclassical scattering amplitude is similar to the exact one, differing only by a constant. To show this point, we first use the WKB approximation for the Coulomb phase-shift (Eq. (5.206)),

$$\sigma_l \simeq \sigma^{\rm WKB}(\lambda) = -\eta + \eta \, \ln \sqrt{\eta^2 + \lambda^2} + \lambda \tan^{-1} \eta/\lambda$$
$$\equiv \eta \, [\ln \eta - 1] - \eta \, \ln \left[\frac{\eta}{\sqrt{\eta^2 + \lambda^2}} \right] + \lambda \tan^{-1} \eta/\lambda.$$

According to Eqs. (3.11a) and (3.11c), we can write

$$\sigma(\lambda) \simeq \eta \, [\ln \eta - 1] - \eta \, \ln \, [\sin(\theta/2)] + \lambda \, \frac{\theta}{2}.$$

With the above approximation, the phase of the scattering amplitude of Eq. (7.154) becomes

$$\alpha(\theta) = 2\sigma(\lambda_0) - \lambda_0\theta - \pi/2 = 2 \, (\eta \, [\ln \eta - 1]) - \eta \, \ln \left[\sin^2(\theta/2) \right] + \pi/2. \qquad (7.156)$$

Now we use the approximation of Eq. (3.88),

$$\sigma_0 = \frac{1}{2} \tan^{-1} \eta + \eta \, [\ln(\eta) - 1] \, ,$$

to write

$$\alpha(\theta) = 2\sigma_0 - \eta \, \ln \left[\sin^2(\theta/2) \right] + \pi - \phi_0, \qquad (7.157)$$

with

$$\phi_0 = \frac{\pi}{2} + \tan^{-1} \eta. \qquad (7.158)$$

Comparing Eq. (7.157) with the exact Coulomb scattering amplitude (Eq. (3.29)),

$$f_{\rm C}(\theta) = -\frac{a}{2\,\sin^2(\theta/2)}e^{-i\eta\ln(\sin^2\theta/2)}\;e^{2i\sigma_0}$$
$$\equiv |f_{\rm C}(\theta)| \times \exp\left[i\left(2\sigma_0 - \eta\,\ln\left[\sin^2\theta/2\right] + \pi\right)\right],$$

we conclude that the phase of the semiclassical scattering amplitude differs from the exact one only by the constant ϕ_0.

Now we come back to the scattering amplitude of Eq. (7.138), which corresponds to the case of sharp cut-off absorption (Eq. (7.137)). We can follow the same steps as in the case of pure Coulomb scattering but keeping in mind that the lower limit of integration is the cut-off angular momentum, $\bar{\Lambda}$, instead of $-\infty$. Eq. (7.147) then becomes

$$f(\theta) = \frac{e^{i\varphi_0 - i\pi/4}}{2k\,\sin\theta/2}\left(\frac{\eta}{\pi}\right)^{1/2}\int_{\bar{\Lambda}}^{\infty}\,d\lambda\,e^{i\Theta_0'\,(\lambda-\lambda_0)^2/2}\,. \qquad (7.159)$$

Accordingly, the integral in terms of the new variable t corresponds to Eq. (7.152) with a different lower integration limit, T. That is,

$$f(\theta) = \frac{e^{i\varphi_0 - i\pi/2}}{2k\,\sin\theta/2}\left(\frac{2\eta}{-\Theta_0'}\right)^{1/2}\left[\frac{1}{\sqrt{\pi}}\int_{T}^{\infty}\,dt\,e^{-t^2}\right]. \qquad (7.160)$$

This limit is related with $\bar{\Lambda}$ through Eq. (7.149), as

$$T = e^{i\pi/4}\left(\frac{-\Theta_0'}{2}\right)^{1/2}\left(\bar{\Lambda} - \lambda_0\right). \qquad (7.161)$$

Note that taking the $T \to -\infty$ limit in Eq. (7.160) one gets the scattering amplitude for pure Coulomb scattering. In this case, the quantity within square brackets becomes equal to one and Eq. (7.160) reduces to Eq. (7.152). Thus, Eq. (7.160) can be written as

$$f(\theta) = f_{\rm C}(\theta)\left[\frac{1}{\sqrt{\pi}}\int_{T}^{\infty}\,dt\,e^{-t^2}\right]. \qquad (7.162)$$

It is convenient to express the lower integration limit in terms of the observation angle, θ, and the grazing angle, $\bar{\Theta}$, which corresponds to the deflection function for the grazing angular momentum, $\bar{\Lambda}$. Using Eqs. (3.11c) and (7.153), and standard trigonometric relations, we get

$$T = e^{i\pi/4}\,\sqrt{\eta}\,\left[\frac{\sin\left(\frac{\theta-\bar{\Theta}}{2}\right)}{\sin\frac{\bar{\Theta}}{2}}\right]. \qquad (7.163)$$
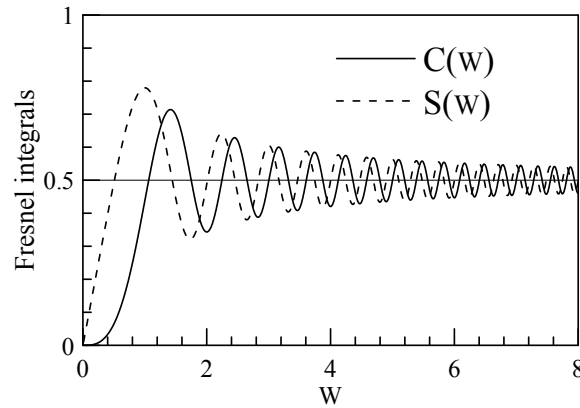
Fig. 7.3   The Fresnel integrals $C(\mathrm{W})$ and $S(\mathrm{W})$.

Usually, the cross section for Fresnel diffraction is expressed in terms of the Fresnel integrals $C(W)$ and $S(W)$, which are real functions of a real argument. They are defined as [Abramowitz and Stegun (1972)]

$$C(W) = \int_0^W dw \, \cos\left(\frac{\pi}{2}w^2\right) \tag{7.164}$$

and

$$S(W) = \int_0^W dw \, \sin\left(\frac{\pi}{2}w^2\right). \tag{7.165}$$

It is clear from the above definitions that these functions are antisymmetric:

$$C(-W) = -C(W) \qquad \text{and} \qquad S(-W) = -S(W). \tag{7.166}$$

The Fresnel integrals are illustrated in figure 7.3. They vanish at $W = 0$ and converge to the limit 0.5 as $W \to \infty$, oscillating around this limit with decreasing amplitudes.

To express the scattering amplitude in terms of Fresnel integrals, we first rewrite Eq. (7.162) as[10]

---

[10]To get the second line of the equation below, we used the value of the Gaussian integral, given in Eq. (7.151).

$$\frac{f(\theta)}{f_{\text{C}}(\theta)} = \left[\frac{1}{\sqrt{\pi}} \int_0^\infty dt\, e^{-t^2} - \frac{1}{\sqrt{\pi}} \int_0^T dt\, e^{-t^2} \right]$$

$$= \frac{1}{2} \left[1 - \frac{2}{\sqrt{\pi}} \int_0^T dt\, e^{-t^2} \right]. \qquad (7.167)$$

The next step is to introduce a new integration variable, w, such that

$$-t^2 \to -i\frac{\pi}{2}\, w^2. \qquad (7.168)$$

This is achieved by the transformation

$$w = e^{-i\pi/4} \sqrt{\frac{2}{\pi}}\, t. \qquad (7.169)$$

Replacing in the above equation $t \to T$, with T given by Eq. (7.163), we obtain the upper integration limit for the new variable:

$$W = \sqrt{\frac{2\eta}{\pi}} \left[\frac{\sin\left(\frac{\theta - \bar{\Theta}}{2}\right)}{\sin\frac{\bar{\Theta}}{2}} \right]. \qquad (7.170)$$

From Eq. (7.169), we have

$$dt = e^{i\pi/4} \sqrt{\frac{\pi}{2}}\, dw \qquad (7.171)$$

and using this result in Eq. (7.167), we obtain

$$\frac{f(\theta)}{f_{\text{C}}(\theta)} = \frac{1}{2} \left[1 - (1+i) \int_0^W dw\, e^{-i\pi w^2/2} \right]. \qquad (7.172)$$

The above result can be expressed in terms of Fresnel integrals (Eqs. (7.164) and (7.165)), as

$$\frac{f(\theta)}{f_{\text{C}}(\theta)} = \frac{1}{2} \left[1 - (1+i)\,(C(W) - i\,S(W)) \right]. \qquad (7.173)$$

Taking the square modulus of the above equation on gets the ratio of the cross section for Fresnel diffraction to the Rutherford cross section. The result can be put in the form

$$\frac{\sigma(\theta)}{\sigma_{\text{Ruth}}(\theta)} = \frac{1}{2} \left[\left(\frac{1}{2} - C(W) \right)^2 + \left(\frac{1}{2} - S(W) \right)^2 \right], \qquad (7.174)$$
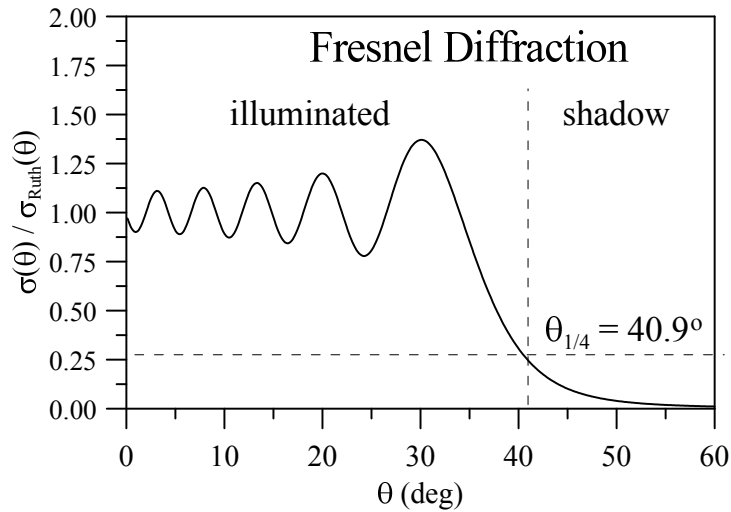
with W given by Eq. (7.170).

Fig. 7.4   Fresnel diffraction within the sharp cut-off approximation. For details see the text.

Fresnel diffraction within the sharp cut-off approximation is illustrated in figure 7.4. The example is the nuclear ^{16}O $+$ ^{208}Pb collision, discussed by Frahn in [Frahn (1966)]. The grazing angle is $\bar{\Theta} = 40.9^{\circ}$ and the Sommerfeld parameter is $\eta = 32.05$. The grazing angular momentum, determined through the Rutherford trajectory, is $\bar{\Lambda} = 86$. Frahn [Frahn (1966)] has shown that the results obtained with the sharp cut-off approximation are in qualitative agreement with the data.

The ratio of the diffractive cross section to the Rutherford one, given by Eq. (7.174), has a very interesting property. At the grazing angle $\theta = \bar{\Theta}$, the argument of $C(W)$ and $S(W)$ is $W = 0$. Thus, the Fresnel integrals vanish and the ratio of the two cross sections takes the simple value of $1/4$. In this way, one can estimate the grazing angle as the scattering angle at which the ratio $\sigma/\sigma_{\text{Ruth}}$ has the value of $1/4$ (see excercise 1, chapter 3).

The angular dependence of $\sigma/\sigma_{\text{Ruth}}$ in Fresnel diffraction is similar to the one in rainbow scattering: oscillatory behavior in the illuminate region, where $\theta < \bar{\Theta}$ ($W < 0$), and decaying in the shadow region, where $\theta > \bar{\Theta}$ ($W > 0$). However, the physics involved in each of these processes is en-

tirely different. Fresnel diffraction is dictated by the imaginary part of the potential whereas rainbow scattering is determined by its real part. In the case of Fresnel diffraction, the shadow region is an immediate consequence of the asymptotic value of the Fresnel integrals, illustrated in figure 7.3. For large positive values of the argument, these functions tend to the limit $1/2$. Therefore, each of the two terms within the square brackets of Eq. (7.174) tends to zero asymptotically and σ/σ_{Ruth} vanishes. The situation is quite different in the illuminated region, where the argument of the Fresnel integrals is negative. Using the antisymmetric properties of Eq. (7.166), for $W < 0$ we can write

$$\frac{\sigma(\theta)}{\sigma_{\mathrm{Ruth}}(\theta)} = \frac{1}{2} \left[\left(\frac{1}{2} + C\left(|W|\right) \right)^2 + \left(\frac{1}{2} + S\left(|W|\right) \right)^2 \right], \qquad (7.175)$$

For large $|W|$, both $C(|W|)$ and $S(|W|)$ oscillate around the value $1/2$, with decreasing amplitude as $|W|$ grows. Therefore the ratio of Eq. (7.175) oscillates around the value 1, with decreasing amplitude for smaller angles, well below $\bar{\Theta}$. This behavior can be observed in the illuminated side of figure 7.4.

More quantitative information about the Fresnel diffraction cross section within the sharp cut-off approximation can be obtained with the help of the asymptotic forms of the Fresnel integrals. Here, we only mention the main results [Almeida and Hussein (1985)]. The first one is the value of the maximum of $\sigma/\sigma_{\mathrm{Ruth}}$, reached at the first maximum below the grazing angle. One finds

$$\frac{\sigma(\theta)}{\sigma_{\mathrm{Ruth}}(\theta)} = 1.4. \qquad (7.176)$$

The second is the approximate expression for the period of oscillation in the illuminated region,

$$\Delta\theta = \left[\frac{2\pi\eta}{\bar{\Lambda}^2 + \eta^2} \right] \frac{1}{\sin\left(\bar{\Theta} - \theta \right)}. \qquad (7.177)$$

The sharp cut-off approximation is a poor description of realistic strong absorption situation. Owing to the step function approximation for the modulus of the S-matrix as a function of angular momentum, the Poisson series converges slowly and terms with $m \neq 0$ should be taken into account in Eq. (5.264).

This shortcoming is eliminated in Frahn's strong absorption model (see e.g. [Frahn (1966); Brink (1985)]). In this model, the modulus of the S-matrix is still expressed in terms of the grazing angular momentum. However, $|S(\lambda)|$ does not jump abruptly from zero to 1, as λ reaches $\bar{\Lambda}$. It varies gradually between these limits over a finite range of angular momentum values, characterized by a *diffuseness* parameter, Δ. The smooth cut-off model for Fresnel diffraction is similar to the one described in the previous section, in the case of Fraunhofer diffraction. Frequently, it is also important to include a small correction in the phase of the S-matrix, arising from the short-range part of the real potential. In [Frahn (1966)], an accurate description of the experimental data for ^{16}O + ^{208}Pb elastic scattering was obtained in this way.

It looks surprising that collisions dominated by the Coulomb field plus strong absorption are analogous to Fresnel diffraction in optics. While in the latter the distance between the source and the scatterer (or the distance between the scatterer and the observation point) is comparable to its size, the situation in atomic and nuclear collisions is completely different. In such cases, the projectile and the target have microscopic dimensions whereas the distance between the source of the incident beam and the target is measured in a macroscopic scale. This suggests that atomic and nuclear collisions could be analogous to Fraunhofer diffraction but not to Fresnel diffraction. The reason for the observed Fresnel pattern is that the Coulomb field deflects the incident particles, producing a focalization effect. This is illustrated in figure 7.5, in the case of a repulsive Coulomb field. The figure shows two classical trajectories with grazing angular momentum. In three dimensions, the emergent grazing trajectories describe a cone and its vertex corresponds to a virtual source, placed close to the scatterer.

7.6   Realistic treatments of elastic scattering with absorptive potentials

In the previous sections we have developed the formal scattering theory of absorptive potentials. In the present section we treat the physical effects inflicted by such potentials on scattering observables. In particular we consider the elastic scattering of neutral and charged particles subject to both real and imaginary interactions, and discuss the qualitative changes that the latter brings on the angular distribution. To be specific, we take

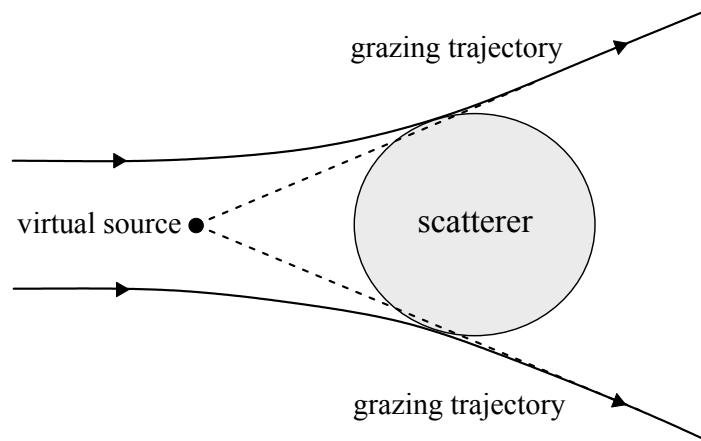344   *Scattering Theory of Molecules, Atoms and Nuclei*

Fig. 7.5   Illustration of the Coulomb focalization effect leading to Fresnel diffraction, which occur, for example, in heavy ion scattering.

the interaction to be,

$$V(r) = U(r) + iW(r) \tag{7.178}$$

The effect of the imaginary part of the potential is to dampen the wave function in the inner region and to supply a sub-unitary S-matrix element, as we discussed before. Besides, it affects the reflection properties in the sense that the real part of the phase shift is modified. This modification in the scattering, can best be seen when analyzing the near- and far-side amplitudes. Although, these amplitudes were introduced and analyzed in chapter 5 using the asymptotic form of the Legendre polynomial, they can in fact be calculated exactly. This can be done through the decomposition of the Legendre polynomial into running waves, as

$$P_l(\cos\theta) = Q_l^{(+)}(\theta) + Q_l^{(-)}(\theta). \tag{7.179}$$

The running waves are defined as [Fuller (1975a)]

$$Q_l^{(\pm)}(\theta) = \frac{1}{2}\left[P_l(\cos\theta) \pm \frac{2i}{\pi}\, Q_l(\cos\theta)\right], \tag{7.180}$$

where $P_l(x)$ is the Legendre polynomial of order l, $Q_l(x)$ is the Legendre function of second kind of the same order and $x = \cos\theta$. For large values

of l and $\cos\theta$ not too close to ± 1, the running waves can be approximated by their asymptotic forms

$$Q_l^{(\pm)}(\theta) \to \left(\frac{1}{2\pi l \sin\theta}\right)^{1/2} \exp\left[\pm i\left((l+1/2)\theta - \pi/4\right)\right]. \qquad (7.181)$$

These approximations were used to derive the semiclassical scattering amplitudes of chapter 5. With the above, the near-side (-) and far-side (+) amplitudes can be calculated exactly, once the radial Schrödinger equation is integrated and the phase shift is extracted as explained in chapter 2. They are then expressed as,

$$f^{(\pm)}(\theta) = \frac{1}{2ik}\sum_{l}^{\infty}(2l+1)\left[|S_l|\,e^{2i\delta_l} - 1\right]Q_l^{(\pm)}(\theta). \qquad (7.182)$$

We observe the important property,

$$Q_l^{(-)}(-\theta) = Q_l^{(+)}(\theta) \qquad (7.183)$$

which results in the identity,

$$f^{(-)}(-\theta) = f^{(+)}(\theta). \qquad (7.184)$$

We remind the reader that both the near-side, $f^{(-)}(\theta)$, and the far-side, $f^{(+)}(\theta)$, amplitudes can be written as an infinite Poisson sum of integrals (see section 5.2.3),

$$f^{(\pm)}(\theta) = \sum_{-\infty}^{\infty} f_m^{(\pm)}(\theta). \qquad (7.185)$$

The presence of absorption will damp most terms in the above sum except, at most, the $m = 0$ and $m = -1$ terms. We then approximate,

$$f^{(\pm)}(\theta) \simeq f_0^{(\pm)}(\theta) + f_1^{(\pm)}(\theta), \qquad (7.186)$$

where the above two terms are integrals in $\lambda = l + 1/2$.

The interference pattern in the calculated angular distribution can best be appreciated with the actual calculation of the near-side and the far-side contributions. Thus, two auxiliary cross sections are introduced,

$$\frac{d\sigma^{(-)}(\theta)}{d\Omega} = |f^{(-)}(\theta)|^2 \qquad (7.187)$$

$$\frac{d\sigma^{(+)}(\theta)}{d\Omega} = |f^{(+)}(\theta)|^2. \qquad (7.188)$$

In collisions of charged particles, the Coulomb contribution to the far-side component of the scattering amplitude tends to be small. This arises from the fact that the integral over angular momentum giving the semi-classical Coulomb far-side amplitude has no stationary points. Thus, in the scattering from Coulomb plus short-range potentials, it should be a reasonable approximation to include the Coulomb contribution fully in the near-side amplitude. However, this is only true for small angles. In fact, Fuller derived explicit expressions for the near- and far-side Coulomb amplitudes [Fuller (1975b)], which are

$$\frac{f_{\rm C}^{(-)}(\theta)}{f_{\rm C}(\theta)} = \frac{1}{1 - e^{-2\pi\eta}} - iC(\eta, \theta) \tag{7.189}$$

$$\frac{f_{\rm C}^{(+)}(\theta)}{f_{\rm C}(\theta)} = \frac{-e^{-2\pi\eta}}{1 - e^{-2\pi\eta}} + iC(\eta, \theta), \tag{7.190}$$

with

$$C(\eta, \theta) = \frac{\left[\sin^2(\theta/2)\right]^{1+i\eta}}{2\pi} \, S(\eta, \theta). \tag{7.191}$$

Above, the function $S(\eta, \theta)$ is given in terms of an infinite series involving the ψ function [Abramowitz and Stegun (1972)]. It is clear that the magnitude of $f_{\rm C}^{(+)}$ is a factor $e^{-2\pi\eta}$ smaller than the near-side Coulomb amplitude, $f_{\rm C}^{(-)}$. This justifies ignoring the former in the near/far calculation in the forward angle region. However, at backward angles the far-side Coulomb amplitude is significant, as it smoothes out the conspicuous, albeit spurious oscillations in the total far-side amplitude.

With the above preliminaries we can identify four types of interference patterns; the near-near (NN), arising from two stationary points of $f^{(-)}$, the far-far (FF), arising from two stationary points of $f^{(+)}$, the near-far (NF), interference of one stationary point of $f^{(+)}$ with one of $f^{(-)}$, and the interference between f_0 and f_1, which we call the Poisson interference pattern (PP). All realistic angular distributions of systems with absorption, can be analyzed within the general scheme of the NN, FF, NF, PP, interference patterns. This can be demonstrated through the realistic calculation to follow.

Let us numerically calculate the elastic scattering of a typical nuclear system, ^{4}He + ^{90}Zr, studied by Put and Paans [Put and Paans (1974)].

We remind that the helium nucleus, i.e. the alpha particle, has 2 protons and 2 neutrons, while Zirconium-90 has 40 protons and 50 neutrons. A phenomenological potential was used by these authors to account for the elastic scattering angular distribution data at several laboratory energies. One of these energies is $E_{\text{lab}} = 79.5$ MeV, which we will discuss below as it exhibits a remnant of a rainbow. The phenomenological nuclear potential in question is $V(r) = U(r) + i\, W(r)$ with $U(r) = U_{\text{N}}(r) + U_{\text{C}}(r)$. The short-range components of the potential, $U_{\text{N}}(r)$ and $W(r)$, are parametrized by the Woods-Saxon shapes

$$U_{\text{N}}(r) = \frac{U_0}{1 + \exp\left[(r - R_r)/a_r\right]}, \quad W(r) = \frac{W_0}{1 + \exp\left[(r - R_i)/a_i\right]}, \quad (7.192)$$

with [Put and Paans (1974)] $U_0 = -140.0$ MeV, $W_0 = -18.7$ MeV, $R_r = 5.50$ fm, $R_i = 7.03$ fm, $a_r = 0.815$ fm and $a_i = 0.575$. The above short-range nuclear potential, the optical potential, is added to the long-range Coulomb potential given by,

$$U_{\text{C}}(r) = \frac{1}{4\pi\epsilon_0} \frac{Z_1 Z_2 e^2}{r}, \qquad\qquad \text{for } r \geq R_{\text{C}} \qquad (7.193)$$

$$= \frac{1}{4\pi\epsilon_0} \frac{Z_1 Z_2 e^2}{2R_{\text{C}}} \left[3 - \frac{r^2}{R_{\text{C}}^2}\right], \qquad \text{for } r < R_{\text{C}}, \qquad (7.194)$$

with $R_{\text{C}} = 5.50$ fm and the atomic numbers $Z_1 = 2$ and $Z_2 = 40$. Thus the full real potential is,

$$V(r) = U_{\text{N}}(r) + U_{\text{C}}(r). \qquad (7.195)$$

For the purpose of understanding the structure of the data and the calculation we first evaluate the real effective potential defined by,

$$U_{\text{eff}}(r, l) = U_{\text{N}}(r) + U_{\text{C}}(r) + \frac{\hbar^2}{2\mu} \frac{l(l+1)}{r^2}. \qquad (7.196)$$

This potential is illustrated in figure 7.6, for a few values of the orbital angular momentum, l. Clearly $U_{\text{eff}}(r, l)$, shows maxima, $U_{\text{eff}}(r_m, l_m)$, at all values of $l \leq 26$. At the energies $E_{\text{c.m.}} = U_{\text{eff}}(r_m, l_m)$, the colliding system exhibits orbiting, as discussed in Chapter 5 (Eqs. (5.404) and (5.405)). The maximum of the $l = 26$ effective potential is very close to an inflection point, indicating that above $l = 26$ the effective potential grows monotonically as r decreases. Thus, $E_c = V(r_c, l = 26)$ is approximately the transitional energy above which orbiting ceases to exist, and the scattering would be

348   *Scattering Theory of Molecules, Atoms and Nuclei*
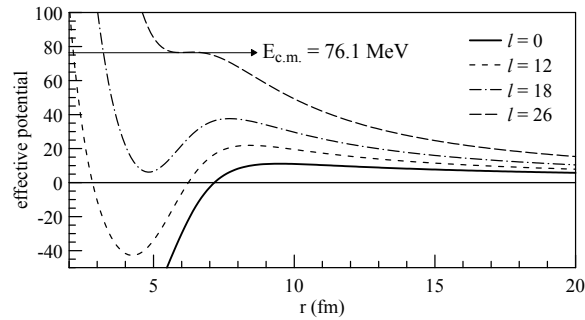

Fig. 7.6   Radial dependence of the effective potential of Eq. (7.196), for the partial-waves $l = 0$, 12, 18, and 26. The collision energy of the detailed discussion in the text is indicated by a horizontal line.
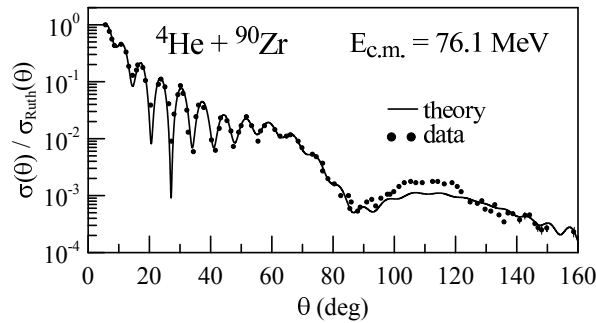

Fig. 7.7   The differential cross divided by the Rutherford cross section at $E_{c.m.} = 76.1$ MeV. The data points are from [Put and Paans (1974)] and the solid line corresponds to a quantum mechanical calculation with the complex potential discussed in the text.

dominated by rainbow.

Now, we compare the theoretical cross section with experimental results. We consider the data of [Put and Paans (1974)], which were taken at several laboratory α particle energies. In figure 7.7, we exhibit the case at $E_{\text{lab}} = 79.6$ MeV or, equivalently, a center of mass energy of $E_{c.m.} = 76.1$ MeV, which coincidentally is very close to the transitional energy, E_c. The agreement between the experimental and the theoretical results is quite rea-

sonable. One sees in the data the NF interference at small angles, followed by damped rainbow oscillations with the first Airy minimum quite conspicuous at 85 degrees. It corresponds to the nuclear rainbow, associated with negative values of the deflection function. As discussed above, the energy here is very close to the transitional energy, and the rainbow is not quite formed as a well behaved minimum in the deflection function. In fact one would expect an almost orbiting case. To demonstrate this we exhibit the classical deflection function for this case in the top panel of figure 7.8. At $l = 26$ one finds an onset of orbiting, though not a singular one ($\theta \to -\infty$). The sharp very deep rainbow/orbiting situation above makes the discussion of the interference patterns of the angular distribution at $E_{\text{c.m.}} = 76.1$ MeV rather complicated.

To avoid this problem, we consider the higher energy of $E_{\text{c.m.}} = 200$ MeV, at which, no orbiting would be present, but just a mild rainbow. This is illustrated in the middle panel of figure 7.8 (indicated by (a)). One observes a rainbow at $\Theta(\lambda) \simeq 51$ degrees for $\lambda_r \simeq 36$. In the bottom panel of the figure (indicated by (b)), we show the absolute values of $|S(\lambda)|$, using the same angular momentum scale on the horizontal axis. Inspecting the λ-dependence of the modulus of the S-matrix, we conclude that the contribution from the stationary points below λ_r should be strongly attenuated by absorption. For comparison, we show also the 200 MeV deflection function and S-matrix in the absence of the Coulomb field (dashed lines).

We now present a detailed discussion of the structure of the angular distribution at $E_{\text{c.m.}} = 200$ MeV, considering four different scenarios:

(1) Scattering with the full potential containing repulsive Coulomb, short-range attractive nuclear and absorptive components.
(2) Scattering with the absorptive potential set equal to zero, $W(r) = 0$.
(3) The short-range nuclear component of the potential set to zero, $V_N(r) = 0$.
(4) The Coulomb potential is turned off to simulate neutral particle scattering.

The differential cross sections for the situations listed above are shown in figure 7.9. The curves in the top panel take into account the Coulomb field whereas in the bottom panel the Coulomb potential is set equal to zero. The angular distribution for the full potential shows very sharp NF interference, followed by the first Airy minimum at $\theta \simeq 25^o$, which cannot be seen clearly
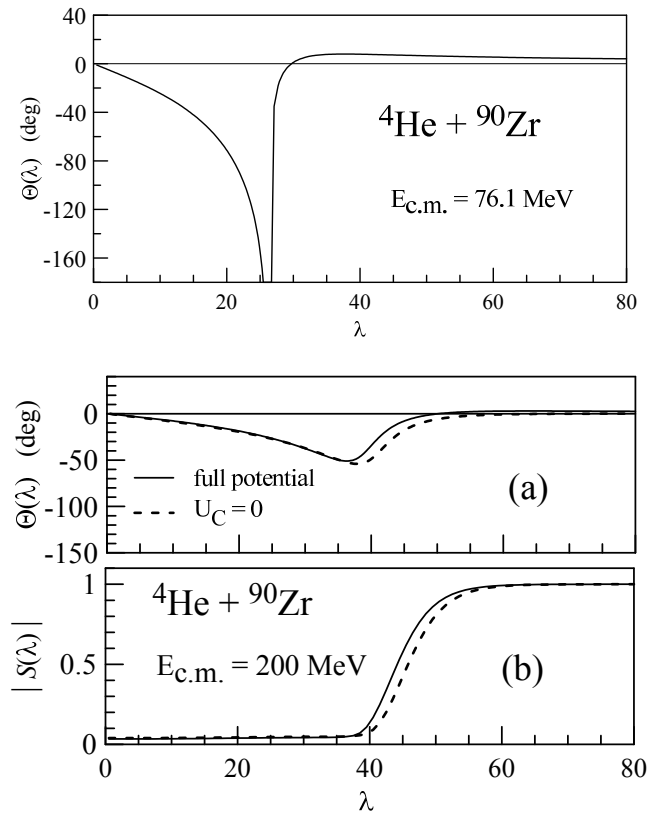
Fig. 7.8   Deflection functions for the ^{4}He + ^{90}Zr system at $E_{\text{c.m.}}$ = 76.1 MeV (top panel) and $E_{\text{c.m.}}$ = 200 MeV (panel (a)). The modulus of the S-matrix at $E_{\text{c.m.}}$ = 200 MeV is shown in panel (b). The dashed lines in the calculations at $E_{\text{c.m.}}$ = 200 MeV were obtained with the Coulomb field switched off.

because this angular region is still affected by the NF oscillations. It then presents the usual drop of the far-side dominated cross section at angles in the shadow region of the nuclear rainbow. Again, an important point to emphasize is the absence of more Airy minima, as compared to the case of atomic scattering with the Lennard-Jones potential considered in chapter 5. This is a consequence of both absorption, which *hides* the inner part of the deflection function, and, when absorption is absent, the smallness of the inner contribution compared to the outer one due to the smaller pre-exponential factor alluded to above, in the former.
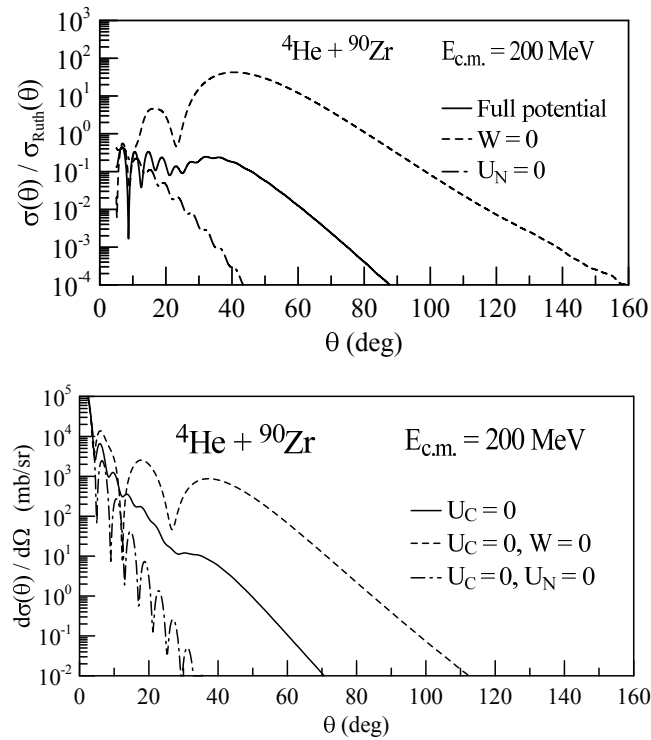
Fig. 7.9   Angular distributions in ^{4}He + ^{90}Zr scattering at $E_{c.m.} = 200$ MeV for the different scenarios listed in the text. On the top panel the Coulomb field is taken into account whereas on the bottom panel it is switched off. The meaning of each curve is indicated in legend of the figures.

The elastic scattering of neutral particles can be discussed by setting the Coulomb interaction equal to zero. Angular distributions for $U_C = 0$ are shown in the lower panel of figure 7.9. The meaning of each curve is indicated inside the figure. Here the case with no absorption comes out similar to the atomic rainbow scattering considered in chapter 5 (see figures 5.14 and 5.15), while the case with both Coulomb and nuclear interactions are turned off, $U_C = U_N = 0$, resembles very much the Fraunhofer diffraction of neutral particles in the smooth-cutoff limit considered in the previous section, and shown as the dashed curve in figure 7.2. Therefore the angular distribution exhibits typical rainbow features in the far-side scattering, while the near side shows the effect of repulsion due to absorption. There

are no NN and strong FF interferences, nor NF interference when the nuclear attraction is turned off.
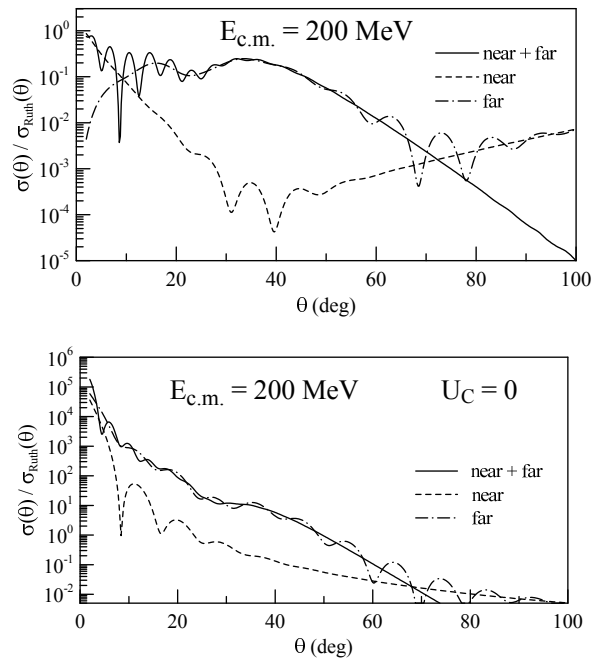

Fig. 7.10   The near/far decomposition of the differential cross section divided by the Rutherford cross section. The energy and the system are the same as in the previous figure and the meaning of each curve is indicated in the legend. On the top panel the Coulomb field is taken into account whereas on the bottom panel it is switched off.

The structure of the angular distribution can be better analyzed if one plots separately the auxiliary cross sections $d\sigma^{(-)}/d\Omega$ and $d\sigma^{(+)}/d\Omega$, of Eqs. (7.187) and (7.188). This is done in figure 7.10. Here, all calculations include both $U_{\rm N}(r)$ and $W(r)$. The results in the top panel take into account the effects of the Coulomb field, whereas those in the bottom panel do not. In the calculations including the Coulomb field (top panel), the near-side cross section dominates at very forward angles, but drops rapidly as θ increases. It reaches a minimum at 40 degrees and then rises at back angles. The far-side cross section, which is small at very forward angles, grows

Scattering from complex potentials 353

rapidly with θ, until it approaches the rainbow region. The two cross sections cross at $\theta \simeq 10$ degrees. Accordingly, the total cross section exhibits very strong NF interference in the neighborhood of $\theta = 10$ degrees. Above this region, the far-side cross section exhibits a typical rainbow pattern damped by absorption and the asymmetrical deflection function. Superimposed on this are the spurious oscillations which would be smoothed out had we included the far-side Coulomb amplitude, as mentioned above and discussed in details by Fuller [Fuller (1975b)]. Thus, the total cross section, contains the NF interference in the forward angle region, and the partial rainbow. There is no FF interference, owing to the absence of orbiting. Studying the cross section in the region where the far-side is dominant, would supply much needed information about the attractive short range nuclear interaction which mostly contributes to the negative branch of the deflection function. An important activity in nuclear scattering research is how to devise a potential that can result in easily identifiable optical scattering pattern. Since W repels, as well as absorbs, one can fiddle with the potential to increase the repulsion and enhance the near-side, while damping the far-side, to make the angular distribution of the desired form. In particular, in many instances one would like to get as close as possible to the Fraunhofer pattern, characterized by the almost equality of $|f^{(-)}(\theta)|$ and $|f^{(+)}(\theta)|$. We leave it as an exercise to find the conditions on the potentials $U_{\rm N}(r), W(r)$ and $U_{\rm C}(r)$, that would lead to perfect equality of these amplitudes,

$$|f^{(-)}(\theta)| = |f^{(+)}(\theta)|. \tag{7.197}$$

A corresponding Near-Far study of the neutral case is shown in the lower panel of figure 7.10. This is simulated setting the Coulomb potential equal to zero. In this case, the cross section is completely dominated by the far-side contribution, arising from nuclear attraction. Once again, one sees the spurious oscillations in the far-side amplitude which would be gone if the far-side Coulomb amplitude were added in the calculation. Further, one sees a practically constant near-side cross section.

Finally, in figure 7.11, we show the absorption cross section, $\sigma_{\rm a}$, for the system as a function of both $E_{\rm c.m.}$ (panel (a)) and $1/E_{\rm c.m.}$ (panel (b)). The full curves represent the absorption cross section for the actual charged system, while the dashed curves are the absorption cross section when the charges are turned off. The charged particle results exhibit clearly the effect of barrier penetration at lower energies, and a practically geometrical
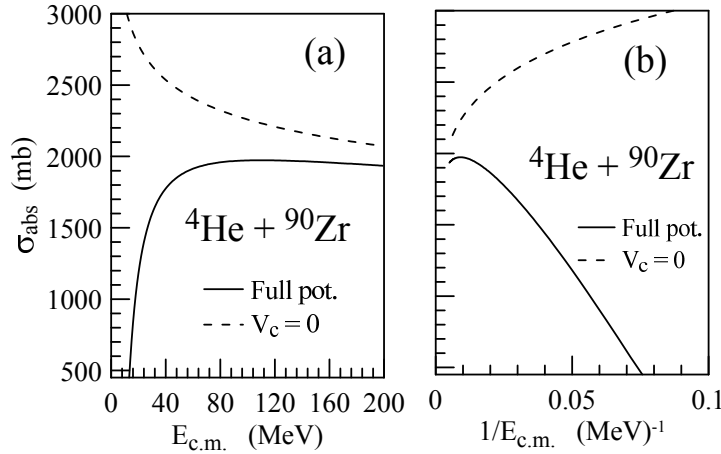
354   *Scattering Theory of Molecules, Atoms and Nuclei*

Fig. 7.11   The absorption cross section in ^{4}He + ^{90}Zr scattering. The cross section is plotted both against $E_{\text{c.m.}}$ (panel (a)) and against $1/E_{\text{c.m.}}$ (panel (b)). The solid lines correspond to calculations including the Coulomb potential whereas the dashed lines were obtained with $V_{\text{C}} = 0$.

behavior at higher energies. In fact the dependence of σ_{a} on $1/E_{\text{c.m.}}$ is practically linear at higher energies. To understand the result, we remind that the absorption cross section is just,

$$\sigma_{\text{a}} = \frac{\pi}{k^2} \sum_{l=0}^{\infty} (2l+1) \left[1 - |S_l(E)|^2\right] = \frac{\pi}{k^2} \sum_{0}^{\infty} (2l+1) \, T_l(E), \qquad (7.198)$$

where $T_l(E) = 1 - |S_l(E)|^2$ is the transmission coefficient. For the charged particle scattering considered here, the Coulomb barrier has an important rôle in absorption. To see this, we consider the parabolic approximation for the barrier, discussed in chapter 5, and consider the effect of W as merely to capture the flux that passes the barrier into the region of attraction. Then, taking the real potential in the barrier region to be approximated by Eq. (5.261), as $V(r) = V_{\text{B}} - 1/2\mu\omega^2 \, (r - R_{\text{B}})^2$, we get for the transmission coefficient the Hill-Wheeler formula (Eq. (5.262),

$$T_l(E) = \frac{1}{1 + \exp\left\{2\pi \left[E - \hbar^2 \, l(l+1)/2\mu R_{\text{B}}^2 - V_{\text{B}}\right]/\hbar\omega\right\}} \qquad (7.199)$$

The calculation of the absorption cross section is made doable by approximating the l-sum by an integral over λ, $l \to \lambda = l+1/2, l(l+1) \to \lambda^2$ (see section 5.2.3)

$$\sigma_{\mathrm{a}} = \frac{2\pi}{k^2} \int_0^\infty \frac{\lambda \, d\lambda}{1 + \exp\left\{2\pi \left[E - \hbar^2\lambda^2/2\mu R_{\mathrm{B}}^2 - V_{\mathrm{B}}\right]/\hbar\omega\right\}}. \qquad (7.200)$$

The above can be evaluated to give what is known as the Wong formula,

$$\sigma_{\mathrm{a}} = R_{\mathrm{B}}^2 \, \frac{\hbar\omega}{2E} \, \ln\left\{1 + \exp\left[\frac{2\pi(E - V_{\mathrm{B}})}{\hbar\omega}\right]\right\}. \qquad (7.201)$$

The above formula for absorption of charged particles has the two desired limits; exponential decrease at energies below the barrier height, and a geometrical behavior at higher energies,

(1) Low energies, $E \ll V_{\mathrm{B}}$, $\ln(1+x) \to x$,

$$\sigma_{\mathrm{a}} = R_b^2 \, \frac{\hbar\omega}{2E} \, \exp\left[\frac{-2\pi|E - V_b|}{\hbar\omega}\right] \qquad (7.202)$$

(2) Higher energies, $E \gg V_{\mathrm{B}}$, $\ln\left[1 + e^y\right] \to y$,

$$\sigma_{\mathrm{a}} = \pi R_{\mathrm{B}}^2 \, \left[1 - \frac{V_{\mathrm{B}}}{E}\right]. \qquad (7.203)$$

Clearly the Wong formula captures most of the salient features of σ_{a}; exponential drop with decreasing center of mass energy, and a linear dependence on $1/E_{\mathrm{c.m.}}$ at higher energies, just as the exact calculation of figure 7.11 (b).

At very low energies, the parabolic approximation is not appropriate and one has to evaluate the absorption of charged particles using the $l = 0$ tunneling of the Coulomb barrier. The exact details of the complex nuclear potential are not important, except for the radius at which it starts acting, R. Once the flux reaches R, absorption sets in and the particle is captured. Then through the use of the WKB tunneling expression of a barrier composed of a $1/r$ potential and a square well at R, we find for the absorption cross section,

$$\sigma_{\mathrm{a}} \simeq \frac{\pi}{k^2} \, T_0(E) = \frac{\pi}{k^2} \, \exp\left[-2 \int_R^{2a} dr \, \sqrt{\frac{2\mu}{\hbar^2}\left(E - \frac{Z_1 Z_2 e^2}{4\pi\epsilon_0 r}\right)}\right], \quad (7.204)$$

where $a = Z_1 Z_2 e^2/4\pi\epsilon_0 E$, is half the distance of closest approach in a head-on collision, introduced in chapter 3. The above can be evaluated in closed form to give,

$$\sigma_{\mathrm{a}} = \frac{\pi\hbar^2}{2\mu E} \, \exp\left\{-2\eta \left[\pi - \sqrt{\frac{R}{2\mu}}\left(1 - \frac{R}{2a}\right) - \sin^{-1}\left(\sqrt{R/2a}\right)\right]\right\},$$
$$(7.205)$$

where $\eta = ka$ is the Sommerfeld parameter (see chapter 3). Since in most cases $a \gg R$, one may approximate the above by,

$$\sigma_{\mathrm{a}} = \frac{\pi \hbar^2}{2\mu E} \; e^{-2\pi\eta}. \tag{7.206}$$

The factor $e^{-2\pi\eta}$ is called the Gamow factor and it plays an important rôle in astrophysically relevant charged particle reactions, where the energies involved are extremely low. We discuss this problem further in section 12.5.

The absorption cross section in the neutral particle case, $U_{\mathrm{c}} = 0$, shown as the dashed curves in figure 7.11, increases with $1/E$, and, at very low energies, shows the well known $1/\sqrt{E}$ ($1/k$ or $1/v$) behavior (see e.g. [Blatt and Weisskopf (1991)]). This behavior is very important in application to thermal neutron capture reactions, the main process used in nuclear technologies. Of course the actual cross section here is full of resonances, called compound nuclear resonances to be discussed in chapter 10. The average cross section, where the resonances are averaged out, can be calculated using complex potential scattering. It is this cross section which shows the $1/k$ behavior. In atomic and molecular systems, the low energy scattering is described by a real potential. However, one does encounter cases where a complex interaction is required. One such case is the elastic scattering of excited molecules encountered in cold gases physics. The absorption in this case is caused by transitions to the ground state of the molecule. The usual effective range description which is employed here, would then require dealing with complex scattering lengths and effective range. We refer the reader to [Balakrishnan *et al.* (1997)] for a more detailed discussion. Similar considerations are used in the description of the scattering of hydrogen from anti-hydrogen [Froelich *et al.* (2000)]. The discussion of [Balakrishnan *et al.* (1997)] and [Froelich *et al.* (2000)] relies on the low-energy form of the scattering amplitude discussed in section 2.11.1, namely,

$$f = \frac{1}{-\frac{1}{a} - ik} = -\frac{a}{1 + ika}. \tag{7.207}$$

The absorption cross section can be obtained from the generalized optical theorem relating the total cross section, σ_{t}, with the imaginary part of the forward scattering amplitude. In the low energy limit, only the s-wave component is relevant and we can write

$$\sigma_{\mathrm{t}} = \sigma_{\mathrm{el}} + \sigma_{\mathrm{a}} = \frac{4\pi}{k} \operatorname{Im}\{f\}. \tag{7.208}$$

Scattering from complex potentials   357

The integrated elastic cross section is then given by $\sigma_{\text{el}} = 4\pi \, |f|^2$. Using this result in the above equation, we get the absorption cross section as

$$\sigma_{\text{a}} = \frac{4\pi}{k} \left(\text{Im}\{f\} - k \, |f|^2 \right). \tag{7.209}$$

In the case of scattering from complex potentials, the scattering length is taken to be complex and we can write

$$a = a_r + i \, a_i. \tag{7.210}$$

Using the above equation in Eq. (7.207), we obtain

$$\text{Im} f = \frac{k \, |a|^2 - a_i}{1 + k^2 \, |a|^2}, \qquad |f|^2 = \frac{|a|^2}{1 + k^2 \, |a|^2} \tag{7.211}$$

and inserting these results into Eq. (7.209) we get

$$\sigma_{\text{a}} = \frac{4\pi}{k} \left[\frac{-a_i}{1 + k^2 \, |a|^2} \right]. \tag{7.212}$$

At low energies, the term in k^2 in the denominator can be neglected and the cross section reduces to

$$\sigma_{\text{a}} = (-4\pi \, a_i) \, \frac{1}{k}. \tag{7.213}$$

Clearly a_i must be negative! The above equation demonstrates the famous $1/k$ law.

The $1/\sqrt{E}$, or $1/k$, low-energy behavior of σ_{a} for neutral particles, is easily seen by considering the $l = 0$ transmission and considering the limit of a complex square well potential with radius R and the complex strength $V_0 = U_0 \, (1 + i \, \chi)$, with χ standing for the ratio of its imaginary to its real part. Using Eq. (2.84) for $\tan \delta_0$, where now δ_0 is complex, the absorption cross section, can be written as,

$$\sigma_{\text{a}} = \frac{\pi}{k^2} \left[1 - \left| e^{2i\delta_0} \right|^2 \right] = \frac{\pi}{k^2} \left[1 - \left| \frac{(1 - i \tan \delta_0)^2}{(1 + \tan^2 \delta_0)} \right|^2 \right], \tag{7.214}$$

where the complex $\tan \delta_0$ is, from Eq. (2.84),

$$\tan \delta_0 = \frac{\frac{k}{K} \tan(KR) - \tan(kR)}{1 + \frac{k}{K} \tan(KR) \tan(kR)}, \tag{7.215}$$

with, $K = \sqrt{2\mu/\hbar^2 (E + V_0(1 + i\chi))}$, and $k = \sqrt{2\mu E/\hbar^2}$. It is an easy matter to show that the absorption cross section behaves as $1/k$ at very

low energy. Further, the above formula for σ_{a} exhibits oscillations as a function of the potential radius, R. This behavior is well known in nuclear physics, and these resonances are referred to as shape resonances. They occur at specific values of R, R_n. The obtention of R_n is left as an exercise (exercise 6).

Exercises

(1) Prove the relation $\left(S^{-1}\right)_{\mathbf{k}',\mathbf{k}} = \langle \tilde{\psi}_{\mathbf{k}'}^{(+)} \, | \, \tilde{\psi}_{\mathbf{k}}^{(-)} \rangle$.

(2) Show that the partial-wave expansion of S^{-1} is

$$\left(S^{-1}\right)_{\mathbf{k}',\mathbf{k}} = \delta(E_{k'} - E_k) \, \frac{\hbar^2}{\mu k} \sum_{lm} Y_{lm}(\hat{\mathbf{k}}')Y_{lm}^*(\hat{\mathbf{k}}) \frac{e^{-2i\delta_l}}{|S_l|}$$

and then go through the details of the derivation of Eqs. (7.101) and (7.102).

(3) Consider the case of pure diffractive scattering within the sharp cut-off approximation for the S-matrix,

$$S_l \equiv |S_l| \, e^{2i\delta_l} \qquad \text{with} \qquad \delta_l = 0 \qquad \text{and} \qquad |S_l| = \Theta(l - \bar{L}).$$

Above, $\Theta(l - \bar{L})$ is the step function at the cut-off angular momentum, $\bar{L} = k\bar{R}$, with $\bar{R}$ representing the radius of the scatterer.

Show that evaluating the partial-wave series for the scattering amplitude one gets,[11]

$$f(\theta) = \frac{\bar{L}}{2ik} \left[\frac{P_{\bar{L}}(\cos\theta) - P_{\bar{L}-1}(\cos\theta)}{1 - \cos\theta} \right] .$$

(4) Calculate the scattering amplitude and the cross section at forward angles, in the case of sharp cut-off absorption. Assume that the cut-off angular momentum is large ($\bar{L} \gg 1$) and that the scattering angle is small enough for the use of the approximation: $P_l(\cos\theta) \simeq J_0(\lambda\theta)$, with $\lambda = l + 1/2 \simeq l$. In this case, the angular momentum can be handled as a continuous variable. Show that the result agrees with the

---

[11] *Hint:* Do not use the semiclassical approximation for the sum over partial-waves. Use the modified expression for the scattering amplitude arising from the recursion relation of Legendre polynomials, given by Eq. (2.55).

one obtained semiclassically[12] (considering only the leading term in the Poisson series):

$$f(\theta) = i\,\bar{R}\,\frac{J_1(\bar{L}\theta)}{\theta} \qquad \text{and} \qquad \frac{d\sigma(\theta)}{d\Omega} \simeq \bar{R}^2 \left[\frac{J_1(\bar{L}\theta)}{\theta}\right]^2.$$

(5) Evaluate the total cross section

$$\sigma_{\mathrm{t}} = \sigma_a + \int \frac{d\sigma(\theta)}{d\Omega}\,d\Omega$$

in the case of sharp cut-off absorption. Then show that the optical theorem, in its version generalized for complex potentials (Eq. (7.24)) is valid.

(6) Calculate the positions of the shape resonances using the expression of Eq. (7.214). Use the approximation $\chi \ll 1$ and thus write $K = K_0 + i\kappa$. With this you should be able to find the condition of maxima in σ_{a}. This then results in the values of the R-resonances,

$$R_n = \left(n + \frac{1}{2}\right)\frac{\pi}{K_0}$$

---

[12] *Hint*: approximate

$$P_{\bar{L}}(\cos\theta) - P_{\bar{L}-1}(\cos\theta) \simeq J_0(\bar{L}\theta) - J_0\left((\bar{L}-1)\theta\right),$$

and use the fist order expansion

$$J_0\left(x + \Delta x\right) \simeq J_0(x) + \left[\frac{dJ_0(x)}{dx}\right]_x \Delta x, \quad \text{and the relation} \quad \frac{dJ_0(x)}{dx} = -J_1(x).$$